NON-STEADY-STATE SOLAR WIND-MAGNETOSPHERE INTERACTION

J. LEMAIRE and M. ROTH

Institut d'Aéronomie Spatiale de Belgique, B-1180 Bruxelles, Belgium

Abstract. Most of the theories proposed to explain the interaction between the solar wind and the geomagnetic field are stationary descriptions based on ideal MHD. In this review an alternative, non-stationary description is discussed. According to this description, most of the plasma-field irregularities, i.e., plasmoids, detected in the solar wind can penetrate inside the geomagnetic field beyond what is considered to be the mean position of the magnetopause. It is the patchy solar wind plasma impinging on the geomagnetic field which imposes rapidly changing and non-uniform boundary conditions over the whole outer magnetospheric surface. This contrasts with the general belief that the observed field variations or 'events' arise sporadically near the magnetopause as the result of some plasma instability.

A brief historical review is given to illustrate the evolution of the theoretical models proposed to explain the interaction of the solar wind with the magnetosphere. The emergence of the idea of 'impulsive penetration' of solar wind plasma irregularities into the magnetosphere is emphasized especially.

A kinetic model of the unperturbed magnetopause is described. This model corresponds to a closed magnetosphere whose surface is a tangential discontinuity. This transition layer can sustain plasma jettings and can be traversed by impulsive penetrating plasmoids. This is against the general belief which considers tangential discontinuities as the worse case with respect to impulsive penetration and plasma jettings.

The mean features of the theory of impulsive penetration are presented. Gusty penetration of solar wind plasmoids depends on their excess momentum density and on the orientation of the IMF. The motion of plasmoids across non-uniform magnetic field configurations (tangential discontinuities) is discussed theoretically. When the dielectric constant of the streaming plasma is large enough for collective polarization effects to become important, an electric field develops which permits cross-B motions of all charged particles as a whole plasma entity. It is re-emphasized that the value of the integrated Pedersen conductivity is a determining factor in cross-B plasma motion. On the other hand, interconnection of interplanetary magnetic field lines and geomagnetic field lines results from collective diamagnetic effects produced by magnetized plasmoids injected into the magnetosphere.

Several consequences of this penetration mechanism are discussed. These are: the escape of energetic particles out of the magnetosphere, the eastward deflection of penetrating plasmoids, the magnetospheric and ionospheric convection patterns, the erosion of plasmoids, and the mass/momentum loading effects.

Some significant experimental geophysical observations supporting the impulsive penetration model are also discussed.

1. Introduction

An impressive number of papers have been written since 1961 on *the Interaction between the Solar Wind and the Magnetic Field of the Earth.* Theoretical manuscripts and presumed experimental 'evidences' for and against one or another type of model have been raining continuously on the desks of Editors of Journals publishing papers in *Space Plasma Physics*.

Beside a large amount of contributed research papers, we have identified over a dozen review papers on this particular topic. Their extended list indicates that, despite this abundant literature and the overwhelming amount of observations which gradually

Space Science Reviews **57:** 59–108, 1991.

became available from ground based stations and from satellites, an unifying physical picture has not yet been accepted by the whole community.

The disparity partly results from the usage of loosely defined words (like: Reconnection, Merging, Viscous-like, ...) which, therefore, have a variety of different meanings to those who are using these frayed words or who are reading these same words.

Furthermore, scientists often like to coin and introduce all kinds of buzzwords! These insightful new words are supposed to mark the group's finding and sometimes a 're-discovery': this might be either new experimental plasma or magnetic field signatures (e.g., FTE, PTE, PLASMOIDS, ...), or a new version of an early theoretical model or idea (e.g., VISCOUS-LIKE INTERACTION, MERGING, RECONNECTION, DISCONNECTION, ...). Unfortunately, many of these exotic names are not used in classical physics lectures nor in plasma physics textbooks, mainly because they lack a clear and standing definition which could make them acceptable to all physicists.

Furthermore, it is regretful that in many instances different buzzwords identify the same class of objects in diverse 'scientific dialects' used by separate groups of our scientific communities. The most customary 'tongues' have their roots in ideal Magnetohydrodynamics (MHD): a very crude approximation of plasma physics theory. Another community, however, is used to argue in terms of kinetic theory.

Most of the theories proposed to describe the interaction between the solar wind and the geomagnetic field are based on ideal MHD; as a consequence many review papers have already been written in this MHD perspective (Axford and Hines, 1961; Axford, 1969; Vasyliunas, 1975; Cowley, 1982; Sonnerup, 1985; Pudovkin and Semenov, 1985; Baumjohann and Paschmann, 1987). For this reason we choose here an alternative description we are more familiar with and more confident of.

In Section 2, after a historical overview outlining the evolution of modelling efforts since 1961, we will address a few general questions that we believe are important starting points. The answers to these questions will be based on relevant laboratory plasma experiments and satellite measurements.

On the rare occasions when the solar wind is stationary and uniform, the unperturbed magnetopause can be considered as a tangential discontinuity. Before discussing the non-steady interaction of the solar wind with the magnetosphere we describe in Section 3 a kinetic model of the unperturbed magnetopause.

In Section 4 we present a summary of the 'impulsive penetration' theory which was often overlooked or misunderstood in earlier reviews, except perhaps in the most recent ones by Lundin (1988a) and Heikkila (1990).

Finally, in Section 5, we shall list significant experimental geophysical observations supporting the Impulsive Penetration Model. Conclusions are summarized in Section 6.

2. Historical Evolution in Modelling Efforts of Solar-Wind-Magnetosphere Interaction

The first model for the interaction of the solar wind with the magnetosphere was proposed in the early sixties (Dungey, 1961), quite before even limited surveys of the whole magnetosphere were available. It was inspired by Giovanelli's (1946, 1947, 1948) original idea that flare optical emissions from atoms are excited by electrons accelerated in induced electric fields near neutral points in the evolving magnetic fields of sunspots. Dungey applied this reconnection model to the interaction of the interplanetary magnetic field with the geomagnetic field; this became the first of an endless series of alternative versions based on the ideal MHD approximation of plasma physics. (In Appendix 1 we recall what was meant originally by 'Ideal MHD'. Indeed, there are many diverse meanings attached to these words.)

Soon after the publication of this first MHD model, another type of MHD interaction model was proposed by Axford and Hines (1961) to describe qualitatively the interaction between the solar wind and the magnetic field of the Earth. This new steady state model became known as the 'viscous-like interaction' scenario.

Because of the lack of decisive observations and the unawareness of relevant laboratory experiments, this field of investigation grew immoderate; for more than twenty years, this question remained open for all kinds of theoretical dissertations and expectations.

MHD descriptions have been much in favour within the space plasma physics community. On the other hand, any of the plasma kinetic approaches based on Chapman and Ferraro (1931a, b, 1932a, b) current model, reviewed in two remarkable articles by Willis (1975, 1978), stayed unpopular and largely ignored.

This field of investigation became the ideal terra to develop a long standing and vivid controversy between two leading schools of thoughts: the open magnetosphere (reconnection/merging type) on one side, and, the closed magnetosphere (viscous-like type) on the other... This controversy lasted almost two decades and it is not yet quite through. The emphasis has changed, however, in the late 1970's, when it appeared that some of the basic assumptions of the early steady state 1-D or 2-D interaction models happened to be disproved by higher time-resolution observations and happened to be too simplistic to properly describe the actual interaction between the solar wind and the magnetic field of the Earth.

Indeed, in both types of models, the solar wind impinging on the geomagnetic field was postulated to be uniform over the whole magnetopause and to change slowly enough so that electrodynamic effects like those advocated by Heikkila (1978a, b, 1982) could be neglected (at least according to the early modellers). Because of their limited time resolution until the late 1970's, solar wind plasma observations were unable to prove or disprove the validity of the quasi-stationnary assumption.

Obviously, ignoring time variations in Maxwell's and Boltzmann's equations makes mathematics a great deal easier, even though it does not necessarily depict the real world correctly!

The attractive advantage of this simplifying assumption being that it reduces the field equations to those of electrostatics and magnetostatics. It brings us conveniently back to the realm of D.C. magnetic and electric fields, and consequently in the idle kingdom of 'magnetic field line topologies' and 'electric equipotential surfaces'. How much easier it is from a mathematical point of view to ignore partial time derivatives! But we must be aware that in doing so we may miss basic electromagnetic effects: electric fields induced locally by rapidly changing magnetic fields or boundary conditions.

However, compelling high time-resolution interplanetary magnetic field and recent plasma measurements indicated that the solar wind plasma is most of the time patchy or inhomogeneous even over distances smaller than one Earth's radius, i.e., smaller than the diameter of the magnetosphere (Turner *et al.*, 1977; Burlaga *et al.*, 1977; Harvey *et al.*, 1979). Therefore, the patchy solar wind plasma impinging on the geomagnetic field necessarily imposes rapidly changing and non-uniform boundary conditions over the whole outer magnetospheric surface.

It is precisely the observation of the irregular nature of the interplanetary magnetic field, by one of us visiting GSFC in 1975, that led to the idea of 'impulsive penetration' (IP) of solar wind plasma irregularities into the Earth's magnetosphere. The high variability observed in all three IMF components over time-scales of seconds (i.e., scale length of 1000–3000 km) was inferred to be due to the presence in the solar wind of small-scale plasma density irregularities convected past the spacecraft with supersonic velocity. Later we called 'plasmoids' these plasma density irregularities or 3-D structures, following Bostick's original definition of 'plasma-field entities' (Bostick, 1956). (See Appendix 2 for the origin of the word Plasmoid.)

At an EGS meeting in Amsterdam on the 'Magnetopause Regions', we proposed in 1976 that these plasma irregularities, which are almost always present in the solar wind, can penetrate inside the geomagnetic field beyond what is considered to be the mean position of the magnetopause. These plasma elements penetrate deeper when they have an excess momentum density with respect to the background solar wind plasma. Collisionless solar wind plasmoids are thrown into the geomagnetic field, just like rain droplets penetrate impulsively through the surface of a lake (Lemaire and Roth, 1978; Lemaire, 1979a). This idea is illustrated in Figure 1(b) showing a series of plasmoids at different penetration depths inside the magnetosphere.

This new scenario led to the first non-stationnary interaction model between the solar wind and the magnetosphere. Heikkila (1982) supported this new mechanism although he described it with a rather different physics.

Prognoz-7 observations of intense magnetosheath-like plasma deep inside the high latitude boundary layer (HLBL or plasma mantle) were interpreted by Lundin and Aparicio (1982) as the indication that solar wind plasma elements can occasionally penetrate the magnetopause and form high-density regions in the plasma mantle. Furthermore, these authors noted that ionospheric ions are accelerated within these high-density plasma regions. Lundin and Aparicio (1982) concluded from these observations that these magnetosheath-like plasma irregularities interact with the ionospheric plasma, and, that their observations support the impulsive penetration theory of solar wind into the Earth's magnetotail lobes. Two years later, Lundin and Dubinin (1984) found also from Prognoz-7 observations definite evidence of magneto-sheath-like plasma density irregularities in the low latitude boundary layer (LLBL) on closed geomagnetic field lines. They attributed them also to impulsive penetration of solar wind plasmoids into the low latitude magnetosphere.

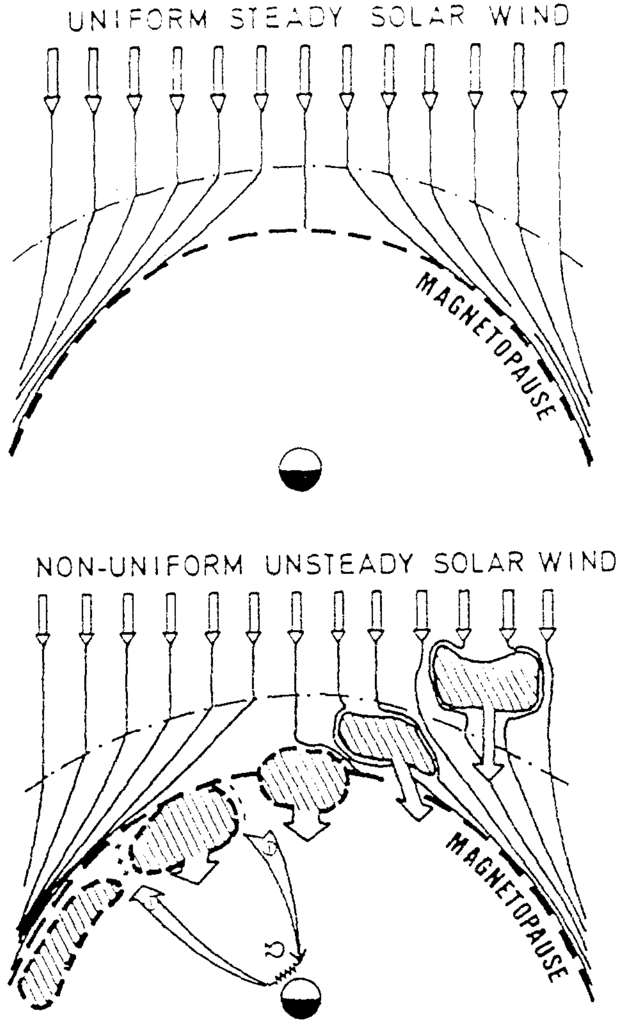

Fig. 1. Equatorial sections of the magnetosphere. (a) When the solar wind is steady and uniform, the magnetopause is a smooth surface along which the solar wind slips without penetration. (b) When the solar wind is non-uniform and unsteady, plasma density irregularities (plasmoids) carried in the solar wind will be able to penetrate deeper in the geomagnetic field provided they have an excess momentum density (after Lemaire and Roth, 1978).

But it was already in the late 1970's that ISEE 1 and 2 results became available, and, that Russell and Elphic (1978, 1979) discovered among a wide variety of magnetic field signatures typical small-scale structures located near the magnetopause. They gave these characteristic magnetic field variations the name: flux transfer event (FTE). Somewhat similar magnetic field signatures were also identified by Haerendel *et al.* (1978) in HEOS-2 data. These distinctive small-scale structures were then called 'inclusions' or 'flux erosion events'. But in retrospect, it became more and more evident to us that these inclusions, flux erosion events or FTE are diverse forms of the diamagnetic plasma irregularities introduced by us in 1976 at the EGS symposium. Bostick (1956, 1957) would have called such plasma-field entities: plasmoids. Such a generic name has the advantage of including not just the special kind of magnetic field signatures now singled out as FTE, but also the whole of many other B-field signatures (and plasma density structures) which are usually seen in the vicinity of the magnetopause region. This is why, subsequently, we adopted the generic name 'plasmoid' to identify all these different types of plasma irregularities.

According to our interpretation, most of the plasma-field irregularities (or plasmoids) detected in the outer magnetosphere and in the magnetosheath are stable *3-D plasma structures* convected in from the solar wind. This contrasts with the believes of others who consider that the observed field variations or 'events' arise sporadically near the magnetopause, like flares, where they would blow up explosively as a result of some local plasma instability.

Thus a new controversy has now replaced the early one about the openness and closeness of the magnetosphere. The latter one has eventually been settled by the consensus that the observations are now showing that the magnetosphere is partially open and partially closed, in accordance with a prediction of the impulsive penetration model.

The current issue under debate is now whether the plasma and field signatures commonly detected on both sides of the magnetopause are explosive events produced locally by some instability, or if they are 3-D plasmoids convected in from the solar wind because of their excess of momentum. This new issue could in principle be settled by coordinated and multi-points measurements in the outer magnetosphere, in the magnetosheath and in the solar wind. The CLUSTER mission should be able to achieve this expectation.

3. The Kinetic Structure of the Magnetopause Tangential Discontinuity

Before we can discuss the non-steady state interaction of plasmoids penetrating into the magnetosphere, we wish to recall first our kinetic model of the magnetopause discontinuity, which is similar to that of the interface between a plasmoid and the ambient background plasma; both surfaces are current layers separating two types of plasma.

On the rare occasions when the solar wind is stationnary and uniform (or almost) the magnetopause can be regarded as a smooth surface along which the solar wind plasma is deflected without penetrating.

Let us assume that the unperturbed magnetosphere is closed and that its surface is a tangential discontinuity in a first approximation.

Since MHD methodologists generally consider the tangential discontinuity case as the worse case with respect to impulsive penetration (Schindler, 1979), we will assume here that the magnetopause is a tangential discontinuity. Anyway there are always places on the 3-D magnetopause surface or at the surface of a plasmoid where this condition is necessarily satisfied. Therefore, we assume that the magnetic field component is zero or small in the Ox-direction normal to the magnetopause surface. This corresponds to the case when the magnetosphere is closed and confined inside a current layer, similar to those envisaged by Ferraro (1952) or Parker (1967) and reviewed by Willis (1975, 1978).

Unlike in the original Chapman–Ferraro layer, the magnetic field intensity in our model of the magnetopause tangential discontinuity does not tend to zero on either side. Furthermore, the direction of **B** changes as a function of x, as illustrated in Figure 2. The magnetic field direction in the magnetosphere (for $x > 0$) is northwards, while for $x < 0$ corresponding to the magnetosheath the **B**-field direction can have any arbitrary direction perpendicular to the Ox-axis. In addition, we assume that the unperturbed magnetosheath and magnetospheric plasmas have no bulk motion in the Ox-direction ($w_x = 0$). Consequently, the component of the external electric field parallel to the magnetopause surface is taken to be zero or negligible: $E_y = 0, E_z = 0$ in the unperturbed magnetopause region.

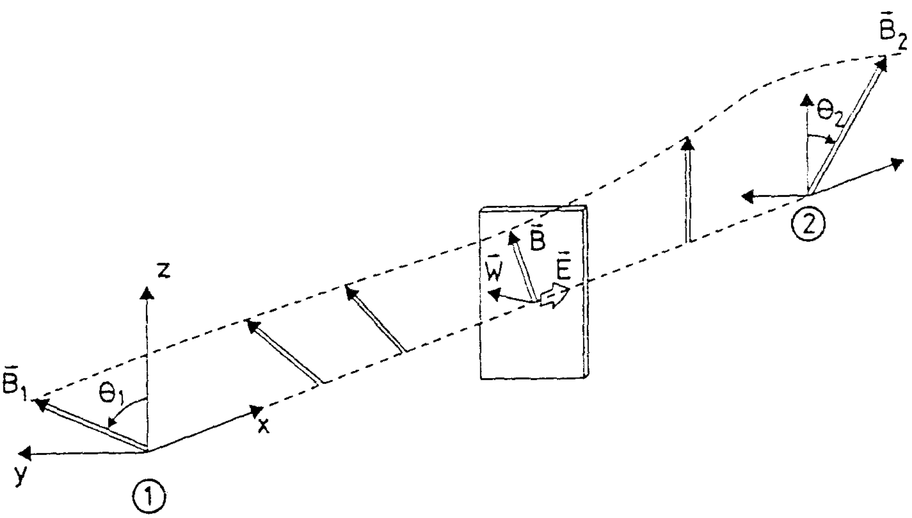

Fig. 2. A three-dimensional representation of the magnetic field vectors along the normal to a tangential discontinuity. This is the way the magnetic field rotates across the magnetopause, when the magnetic field direction in the magnetosheath differs from that in the magnetosphere. In this figure, **B** is the magnetic field vector, **w** is the plasma flow vector and **E** is the electric field vector.

The presence of a normal electric field component within the transition layer implies that there is a charge separation electric field in the interface region between the hot magnetospheric plasma and the denser magnetosheath plasma. Indeed, in the middle of such transition regions where the magnetic field direction as well as the plasma density or/and temperature change rapidly, the electrons tend to separate from heavier ions which have a larger gyroradius. This natural tendency for charge separation due to thermal effects, sets up a polarization charge density which preserves quasi-neutrality within the plasma (Sestero, 1964, 1965, 1966; Roth *et al.*, 1990). This charge separation has been studied in the case of different space plasma current layers like the plasmapause (Roth, 1976), the solar wind tangential discontinuities (Lemaire and Burlaga, 1976; Roth, 1986) and the structure of the magnetopause tangential discontinuity (Roth, 1978, 1979, 1984; Lee and Kan, 1979; Whipple *et al.*, 1984).

The peak intensity of the charge separation electric field in the magnetopause region can vary between a few tens and a few hundreds of mV m^{-1}, depending on the characteristic thickness of the current sheath and the electron and ion temperature on both sides.

Figures 3 and 4 illustrate the plasma bulk velocity distribution within the magnetopause as calculated by Roth (1979). Figure 3 represents the three-dimensional variation of the bulk velocity vector across the inner edge of the magnetospheric plasma boundary layer. In this case, the magnetic field does not change direction throughout the transition layer and is oriented along the Oz-axis, i.e., northwards. The components of the flow are illustrated in Figure 4. Although the component of the bulk velocity parallel to the magnetic field direction, w_z, decreases uniformly from 150 km s^{-1} in the plasma boundary layer to 20 km s^{-1} in the magnetosphere, the perpendicular component, w_y, increases very sharply and reaches a peak value of nearly 400 km s^{-1} in the center of the current layer. This peak value of the perpendicular plasma bulk velocity ($w_y = \Sigma n_i m_i v_{yi} / \Sigma n_i m_i$) is mainly due to the flow of ions across magnetic field lines. In this example, the peak ion flux is associated with a peak of the magnetization current which is proportional to the gradient of the magnetic pressure. Therefore, the ion flux and ion bulk velocity both take a peak value at the location where the gradient of $B^2/(2\mu_0)$ is maximum.

The order of magnitude of this perpendicular flow velocity (400 km s^{-1}) is compar-

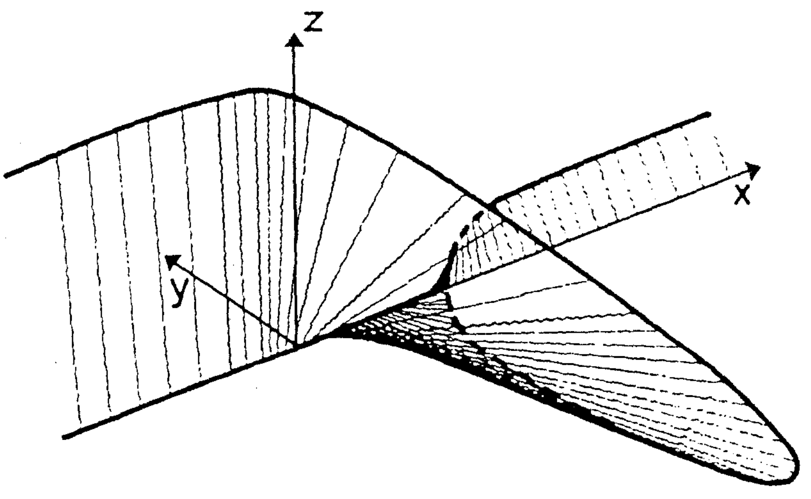

Fig. 3. Three-dimensional representation of the plasma mean bulk velocity **w** parallel to the surface of the tangential discontinuity illustrated in Figure 2. The variation of **w** is shown along the Ox-axis which is normal to the magnetopause. The length of the y-axis and the length of the z-axis represent respectively 125 km s^{-1} and 175 km s^{-1}. The length of the Ox-axis is 205 km. Note the large peak velocity (400 km s^{-1}) in the middle of the current layer. This corresponds to plasma jetting along the magnetopause (after Roth, 1979).

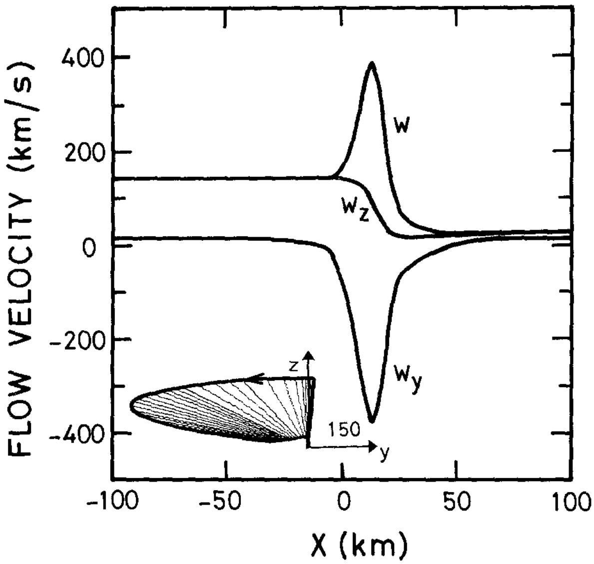

Fig. 4. Amplitude (w), y-component (w_y), and z-component (w_z) of the flow velocity across the inner edge of the plasma boundary layer. The hodogram in the left lower corner shows that the flow velocity has rotated through an angle of more than 90°. The length of the y-axis represents 150 km s^{-1}. The parallel component (w_z) decreases monotonously from 144 km s^{-1} to 26.4 km s^{-1}, while the perpendicular component has a peak of 400 km s^{-1} near $x = 0$ due to the intense ion current density. All the plasma components have the same asymptotic perpendicular mean velocities equal to 17 km s^{-1} (after Roth, 1979).

able to that observed by Paschmann *et al.* (1979) in regions where they detected plasma jetting. These observations are often quoted as evidence for steady-state reconnection or quasi-steady-state merging at the magnetopause. But as demonstrated by Figure 4, these observed plasma jettings can equally well be reinterpreted as the consequence of (i) large grad-B and (ii) large values of **E** resulting from localized peaks of the charge separation electric field in the middle of a magnetopause tangential discontinuity. This alternative explanation of plasma jetting based on kinetic plasma theory was proposed by Roth (1981) at the 4th IAGA Scientific Meeting (Edinburgh). This alternative interpretation does not imply the existence of any reconnection line, nor any X-line, nor any localized diffusion region where anomalous plasma processes have to be postulated. On the contrary our explanation of plasma jetting is based on plain kinetic theory of fully-ionized gases.

Similar peaks of the charge separation electric field intensity E_x and similar localized plasma jetting events are expected at any sharp interface between plasmoids and the background plasma in which they are moving: i.e., within the current layer separating the inside and the outside of solar wind plasma irregularities.

The interface between the magnetosphere and the external plasma (or the interface between a plasmoid and its background) can also be a rotational discontinuity. In this case magnetic field lines cross the interface surface as illustrated in Figure 5. To maintain quasi-neutrality of plasma and satisfy Poisson's equation an electrostatic double layer forms at the point where the magnetic field lines penetrate through the

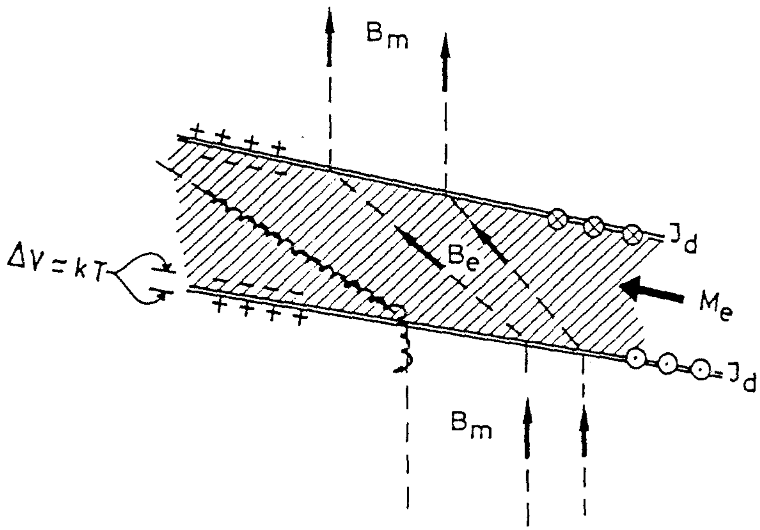

Fig. 5. Schematic representation of a cylindrical plasma element engulfed in an external magnetic field ($\mathbf{B}_m$). The magnetisation ($\mathbf{M}_e$) produced by the surface currents ($\mathbf{J}_d$) is not anti-parallel to $\mathbf{B}_m$. The magnetic induction $\mathbf{B}_e$ inside the filament is not aligned with $\mathbf{B}_m$. The dashed lines represent magnetic field lines traversing the boundaries of the plasma element. Note that, unlike in certain drawings of FTE, the plasma filament does not coincide with a magnetic flux tube. The electrons inside the plasmoid are prevented to escape across the boundaries by electrostatic potential barriers which preserve global quasi-neutrality within the plasma density enhancement. The excess plasma pressure inside the plasmoid can produce a field aligned expansion of the volume element (after Lemaire, 1979a; see also Farrugia *et al.*, 1987).

surface of discontinuity (see Lemaire and Scherer, 1978). This double layer produces a parallel electric field whose peak value depends on the electron temperatures on both sides.

But in any case this thermoelectric potential distribution along the magnetic field lines invalidates locally the ideal MHD assumption: $\mathbf{E} \cdot \mathbf{B} = 0$ or $\mathbf{E}_{\|} = 0$. By the same token it invalidates one of the hypothesis used to demonstrate the frozen-in-field theorem in MHD plasma physics (see Appendix 1).

This is one of the reasons why we consider that ideal MHD leads to erroneous conclusions, when it is applied without discrimination by assuming that magnetic field lines in collisionless plasmas are necessarily equipotential lines.

4. What Is the Impulsive Penetration Theory All About?

4.1. Preliminaries and Prerequisites

The theory of impulsive penetration has been explained in a series of papers (Lemaire and Roth, 1978; Lemaire, 1977, 1979a, b, Lemaire *et al.*, 1979). The latest contributions of it can be found in Lemaire (1985, 1987, 1989).

Before we outline the main features of the theory of impulsive penetration the reader should examine some relevant articles describing results from laboratory plasma experiments obtained by Bostick (1956, 1957), Baker and Hammel (1962, 1965), Wessel *et al.* (1988), as well as by Demidenko *et al.* (1966, 1967, 1969, 1972).

All these enlightening experiments deal with plasmoids injected impulsively across uniform or non-uniform magnetic fields (see Appendix 2 for the origin of the word 'plasmoid'). A thorough examination of these laboratory experiments is a most instructive exercise which prepares adequately to what will be said in the following sections. The relevance of these laboratory plasmoid results to the problem of solar wind magnetosphere interaction has been discussed recently in some details by Lemaire (1989).

But there are also other sets of observations that the reader should be acquainted with: the high resolution interplanetary magnetic field measurements like for instance those of EXPLORER 43 which one of us has had the privilege to analyse in 1975 at the Laboratory for Extraterrestrial Physics/GSFC. These magnetic field measurements (25 vectors measured each second of time) definetely show that the solar wind plasma is non-uniform (irregular) over distances less than one Earth's radius. To become aware of this initial fact is a prerequisite preparing adequately to follow the description of the IP theory.

These high-resolution magnetic field observations indicate that almost all the time there are small directional changes in the IMF components similar to those analysed by Burlaga *et al.* (1977). It is unusual to find in high resolution magnetograms periods of more than 30 s of time when all three components do not change by at least a few percent. There are also, but less frequently, field variations with much larger amplitudes (see Burlaga *et al.*, 1977; Turner *et al.*, 1977). The frequent small changes of B_x, B_y, or B_z are evidence that small-scale electric currents are flowing nearly everywhere inside the solar wind plasma which is convected over the spacecraft.

This system of small-scale currents is the manifestation of small scale plasma inhomogeneities, i.e., of plasma density or/and temperature gradients in the solar wind. But because of the rather low time resolution of early plasma particle measurements (one value every 1 to 3 minutes), the solar wind plasma was generally regarded as rather uniform over distances larger than the diameter of the magnetosphere.

But, since 1978–1979 when ISEE 1 and 2 provided much higher time-resolution plasma data, small-scale plasma density irregularities have been undisputably identified in Harvey's observations obtained from the wave propagation experiment (Harvey *et al.*, 1979; Celnikier *et al.*, 1983, 1987).

In short, what should be remembered in order to appreciate what follows? We believe it is a prerequisite to know that the experimental evidences quoted above indicate that:

(i) the solar wind plasma is almost never uniform over distances of the order of the diameter of the magnetosphere: i.e., that the supersonic solar wind flow is a mess of small scale plasmoids;

(ii) collisionless plasma irregularities (laboratory plasmoids) with an excess of momentum can freely propagate across magnetic field lines (even across non-uniform or sheared magnetic fields), provided that these field lines are coupled to walls (or an ionosphere) where the value of the transverse Pedersen conductivity is finite and not too large.

With these prerequisites in mind we can now proceed to the description of the theory of impulsive penetration (IP) proposed by Lemaire and co-workers.

4.2. Impulsive Penetration of a Plasmoid into the Magnetosphere

In Section 3 we have described the kinetic structure of a stationay current layer separating the plasma inside a plasmoid (or inside the magnetosphere) and outside of it.

Let us now examine what happens when the solar wind is not uniform and not stationary, but formed of small-scale plasma density irregularities. This is illustrated in Figure 1(b). What happens to these plasma clouds when they approach a stationary magnetopause surface like that described in the previous paragraphs?

4.2.1. *Excess Momentum Density, and Penetration Velocity*

Let us follow one of these many plasma density enhancements ($\Delta n > 0$) moving in the Ox-direction with the background solar wind speed (w). If this 'plasma-magnetic entity' corresponds to an excess density but has the same bulk velocity as the surrounding solar wind background, its momentum density, $(n + \Delta n)mw$, in the Ox-direction is then necessarily larger than the average (nmw).

This plasma element will conserve its excess momentum after it has passed through the magnetospheric bow shock. Therefore, it can plough its way through the magnetosheath with a larger speed than the decelerated average solar wind plasma. Unlike the other plasmoids which have a lower momentum density than average, the former one will reach the position of the mean magnetopause with an excess momentum and an excess kinetic energy. At the mean magnetopause position, where the normal component of background magnetosheath plasma velocity becomes equal to zero, the plasmoid has a residual velocity (v_e) given by

$$v_e = w\Delta n/(n + \Delta n)\,. \tag{1}$$

4.2.2. *The Magnetopause Is Not an Impenetrable Surface!*

Most MHD methodologists would consider that the plasma element could not traverse the surface of the magnetopause, but that it would only deform it as if the magnetopause would be a rubber membrane or a transparent plastic surface. Of course, the magnetopause is nothing like a 'material plastic membrane' which would be impenetrable for plasmoids. The magnetopause is just a continuous region separating the magnetosheath from the magnetosphere.

Schindler (1979) has argued from an MHD point of view that filamentary plasma elements can only penetrate in the magnetospheric cavity when the magnetic field inside these plasmoids is either parallel or anti-parallel to the northward magnetospheric field. He considered infinitely long solenoidal filaments which necessarily have an infinite self-induction coefficient. To change the magnetic field inside these infinitely long solenoids, an infinite energy is needed. Furthermore, Schindler (1979) ignored electrostatic double layers and the existence of charge separation E-fields both perpendicular and parallel to the magnetic field direction. The existence of a finite parallel E-field invalidates the MHD approximation at the surface of oblique cylinders as illustrated in Figure 5. But, real plasmoids are never infinitely long objects, nor ideal MHD objects.

Sometimes it is difficult, from high-resolution magnetic field measurements, to identify where exactly the magnetopause transition occurs along the trajectory of a spacecraft. Indeed, there are cases when neither the magnetic field intensity nor its direction change significantly when the magnetometer moves out of the magnetosphere (Eastman, 1979). This occurs at the frontside magnetopause when the IMF is northward and when magnetosheath plasma has a low β-value. Under these circumstances, a plasma density irregularity approaching the Earth with an excess momentum density does not feel any 'magnetic field barrier'. The plasmoid cannot 'tell' whether or not it is crossing magnetic field lines which are 'open' or 'closed', 'reconnected', 'disconnected' or 'interconnected' ... Indeed, sensing the local B-field intensity and direction does not tell to the penetrating plasmoid (nor to a magnetometer) what is the shape and span of the magnetic field lines at some distance. The plasmoid will not really care whether it is on 'closed' geomagnetic field lines or still on 'open' interplanetary ones. It will proceed and eventually penetrate in a region where the magnetic field lines are connected (coupled) to a resistive ionosphere. The magnetic field intensities being the same on both sides of the magnetopause, the plasmoid moves across this transition layer with a constant velocity. The polarization electric field which builds up inside the plasma element to keep it moving, is similar to that measured by Bostik (1956, 1957), Baker and Hammel (1962, 1965) or Demidenko *et al.* (1966, 1967, 1969, 1972) in their laboratory experiments. This electric field is also the same as that inferred by Schmidt (1960) for uniform and non-uniform B-field distributions.

When the magnetic field has neither the same direction nor the same intensity on both sides of the magnetopause, a similar electric field builds up inside the plasmoid and in its vicinity to keep it moving. But in this case its bulk velocity will change adiabatically across the boundary as a result of the change in the magnetic field intensity and direction (Lemaire, 1985) (see Section 4.2.6).

A parent interpretation is that of Miura (1987) who considers that Rayleigh–Taylor instabilities develop at the magnetopause surface. This would then push plasma tongues through the magnetopause. The penetration mechanism envisaged by Miura (1987) is basically similar to that considered in our theory of impulsive penetration. The essential difference between both interpretations resides in the origin of these plasmoids: according to Miura they should be formed locally by an MHD Rayleigh–Taylor type instability, while we argue that they are plasma irregularities brought in from the solar wind through the bow shock and magnetosheath. Similar arguments can be developed about the Kelvin–Helmholtz instability, comprehensively reviewed by Belmont and Chanteur (1989).

Another parent interpretation is that of Heikkila (1982) who argues also with us that the plasmoids have indeed their origin in the solar wind: i.e., that they do not necessarily result from local MHD instabilities at the magnetopause. The main difference between his interpretation of the impulsive penetration mechanism and ours resides in a possible contribution of induced electric fields (classically defined as $\mathbf{E} = -\partial\mathbf{A}/\partial t$) in addition to the polarisation electric fields ($\mathbf{E} = -\text{grad}\,\phi = -\mathbf{v}_e \wedge \mathbf{B}$) that we introduced originally. Furthermore, his penetration scenario holds only in the case of a southward IMF, and requires for the unperturbed magnetopause a non-zero **B**-field normal component. Finally, Heikkila did not consider non-adiabatic braking of plasmoids resulting from electric coupling to the resistive ionosphere as a primordial physical process. It should be pointed out that the induced electric fields which were introduced by Heikkila (1982) can indeed have an intensity comparable to that of the polarisation electric field when the plasma-β is of the order of unity. However, in the case of low-β plasmas, induced electric fields play a relatively minor role.

4.2.3. *Finite Integrated Pedersen Conductivity and Non-Adiabatic Braking of Plasmoids*

Once the plasmoid has reached the region behind the mean position of the magnetopause it moves eventually across closed* geomagnetic field lines; it will then be slowed down non-adiabatically, like the plasma streams injected in Baker and Hammel's plasma experiment when the walls of the vacuum chamber are good electrical conductors. Like the walls in these laboratory plasma experiments, the Earth's ionosphere is an electric load coupled to the moving plasmoid via magnetic field lines whose parallel conductivity is extremely large but whose transverse Pedersen conductivity (Σ_p) always has a finite value at low altitudes.

The major contribution to the integrated Pedersen conductivity comes from the E-region where the ion gyrofrequency is comparable to the ion-neutral collision frequency. The integrated Pedersen conductivity of magnetic field lines extending to the magnetopause or polar cusps ranges from 0.2 to 10 mho depending on the solar zenith angle (see the comprehensive review by Brekke and Hall, 1988).

Why is the value of the integrated Pedersen conductivity of such importance for plasma streams in the laboratory experiments (as demonstrated by Baker and Hammel, 1965) and for solar wind plasmoids injected into the magnetosphere? The reason is

* Since there are no magnetic monopoles all magnetic field lines are closed lines; it has been a plague to introduce the concept of open magnetic field lines. It was introduced in the early days of MHD to sketch whether particle guiding centers are able to penetrate inside the magnetosphere along reconnected or interconnected magnetic field lines. But it must be recalled that drawing sophisticated magnetic field lines topologies alone cannot tell anybody where plasma particles are going to drift eventually. Because of gradient-B and curvature drifts, the charged particles with non-zero energy do not follow the magnetic field lines. In addition to the gradient-B and curvature drifts, particles experience the electric drift which can be vanishingly small or arbitrarily large depending on the electric field distribution which is applied in the direction perpendicular to **B**. In other words specifying a magnetic field lines topology is useless if the electric field lines or equipotentials are not given at the same time. Since the electric field distribution is not uniquely determined when a set of magnetic field lines is given, we consider that the magnetostatic description generally used to illustrate plasma motion or plasma convection is incomplete and, therefore, misleading. This misconception is related to the unnecessary concept of 'magnetic field lines motion' introduced in plasma physics by Alfvén for very specific laboratory conditions: e.g., to describe the flow of highly conducting fluids like mercury in laboratory experiments. But it has been a slip to apply this frozen-in-field concept in all collisionless plasma cases.

simply that the polarisation electric field inside the moving plasma element (which keeps it moving), as well as the electric field in its surroundings (which deflects the magnetosheath or magnetospheric plasma around the intruding plasmoid) are quickly short-circuited when the integrated Pedersen conductivity is large. This fact is illustrated in Figure 6. When Σ_p is large all electric potential gradients inside and in the vicinity of the plasma stream quickly decrease to zero. The convection electric field becomes vanishingly small and the bulk speed ($\mathbf{E} \wedge \mathbf{B}/B^2$) of the plasma inside as well as outside the moving plasmoid quickly slows down to zero.

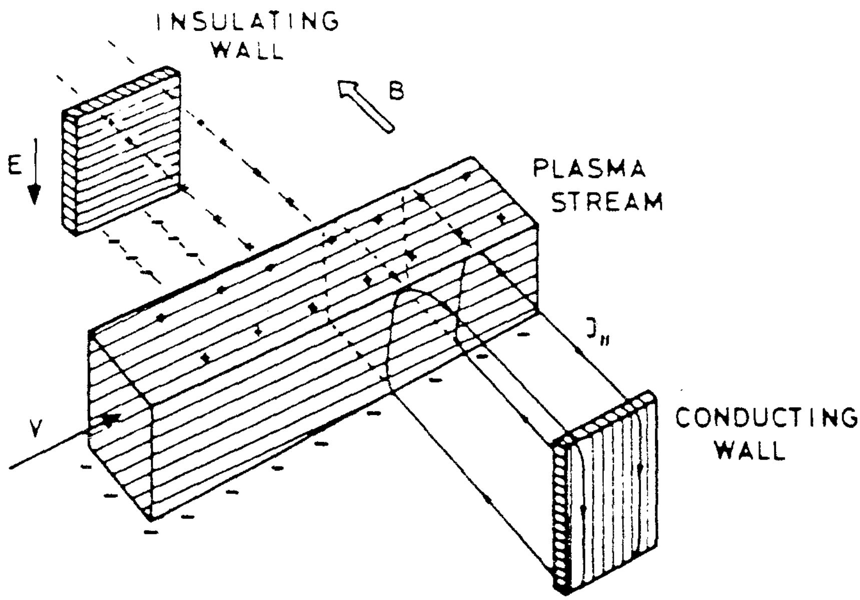

Fig. 6. Simplified model of a collisionless plasma crossing a uniform magnetic field showing first, the charging up effect of an insulating wall and secondly, the depolarizing effect of a conducting wall. In the first case the plasma stream keeps flowing across magnetic field lines with a constant velocity. In the second case the plasma stream is uniformly decelerated. Its excess kinetic energy is then dissipated by Joule heating in the walls (after Baker and Hammel, 1965).

Lemaire (1977) calculated that for $\Sigma_p = 0.2$ mho a solar wind plasmoid with an excess density $\Delta n/n = 5\%$, moving in the solar wind with a velocity $w = 400$ km s^{-1} and which has a characteristic scale length $l = 10\,000$ km, is slowed down in about $t_1 = 30$ min. Its maximum penetration distance is then $\Delta x = 2\,R_E$ behind the average magnetopause position. If the value of the integrated Pedersen conductivity would be 10 times larger, then the non-adiabatic slowing down time and the maximum penetration depth would both be reduced by a factor of 10: i.e., the plasma element would not penetrate very deep into the geomagnetic field.

The kinetic energy of the injected plasmoid is dissipated by Joule heating in the conducting walls of the vacuum tank or in the resistive dayside cusp ionosphere. The excess momentum of the injected plasma element is transferred to the walls and to the ionosphere in the high latitude 'trough regions'. This is how we explain that plasmoids penetrating in the dayside low-latitude plasma boundary layer drive ionospheric convection from the trough regions northward over the polar caps (Lemaire, 1979b). Note that part of the momentum and energy of the plasmoid is also transferred to the ambient gas in the plasma chamber or in the magnetosphere (Bostick, 1956; Lundin, 1988a).

4.2.4. *Conservation of Magnetic Moment and Adiabatic Deceleration*

In addition to this non-adiabatic (irreversible) slowing down mechanism, a plasmoid penetrating in the magnetosphere can be decelerated adiabatically when the magnetic field intensity inside the magnetosphere is larger than in the magnetosheath. Conversely, it is accelerated adiabatically when the magnetic field intensity is smaller in the region wherein it penetrates.

To our knowledge, it is Schmidt (1960) who first gave a theoretical demonstration of this fact which has been proven since by laboratory experiments like those of Demidenko *et al.* (1966, 1967, 1969, 1972). In these laboratory experiments the magnetic field intensity is non-uniform: B increases along the Ox-axis, like the geomagnetic field intensity.

As a result of adiabatic conservation of the magnetic moment of its particles, the plasmoid as a whole is decelerated when it penetrates in a region where the value of B is enhanced. The reason is that the energy of the particles perpendicular to $\mathbf{B}$ increases such that $v_\perp^2/B$ is conserved; this enhancement of the perpendicular thermal energy is achieved at the expense of the initial kinetic (convection) energy. As a matter of consequence, the kinetic energy ($nmv_x^2/2$) of this ensemble of particles decreases until its momentum density in the forward direction vanishes, i.e., until the center of mass of the plasmoid eventually is stopped (see Equation (3) below).

4.2.5. *Electric Field and Plasmoid Velocity*

As a consequence of oppositely directed Larmor gyration and polarisation currents for electrons and ions, the ions tend to form a positive space charge along one of the lateral surfaces of the moving plasmoid, while the electrons build up a negative surface charge on the opposite side as described by Schmidt (1960). This produces inside the plasma element a transverse polarisation electric field $\mathbf{E}$ whose value is precisely equal to

$$\mathbf{E} = -\mathbf{v} \wedge \mathbf{B}, \tag{2}$$

where $\mathbf{v}$ is the bulk velocity of the center of mass, and $\mathbf{B}$ the intensity of the local magnetic induction inside the plasmoid.

From the Lorentz transformation it comes that, in the frame of reference comoving with the center of mass, the electric field intensity, $\mathbf{E}' = \mathbf{E} + \mathbf{v} \wedge \mathbf{B}$, is equal to zero. To simplify the problem, we ignore here possible eddy motions inside the plasmoid itself like those sketched in Figure 7. This additional possibility is beyond the scope of the present review. Like in hydrodynamics there is a variety of different internal motions

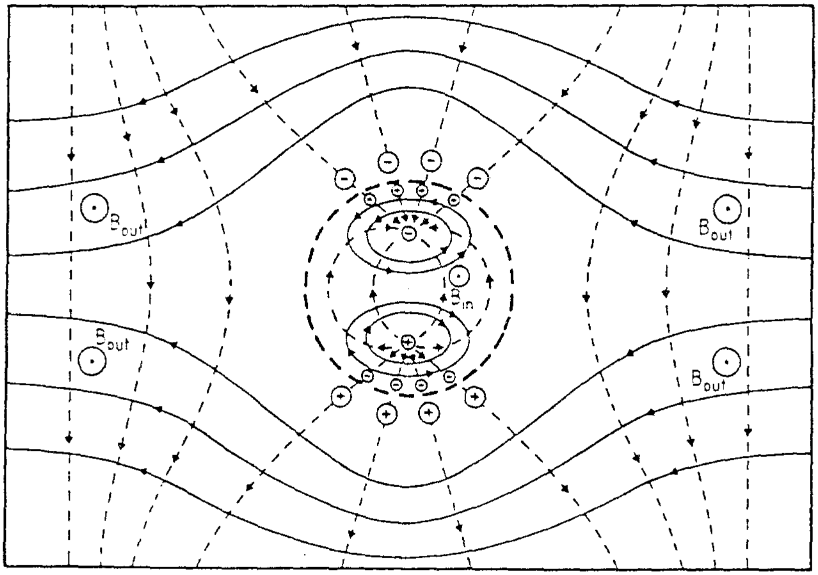

Fig. 7. The short dashed circle represent the cross section of a spherical plasmoid in an external magnetic field ($\mathbf{B}_{out}$). The plasma structure moves to the right with a constant bulk velocity $\mathbf{v}$. The plasma outside is streaming around the plasmoid along the solid lines, with a velocity $\mathbf{E}_{out} \wedge \mathbf{B}_{out}/(B_{out})^2$. The long dashed lines are electric field lines. As a result of the polarisation charges at the surface of the spherical plasma eddy, a dipole electric field $\mathbf{E}_{out}$ is created outside. Inside the plasmoid, two convection cells have been drawn, as one of many possible flow patterns.

in each plasmoid. We will only be concerned here with the mean bulk motion, ignoring, therefore, all kinds of possible vortex motions within the moving plasmoid.

Considering that the magnetic moments (μ) of all plasmoid particles are adiabatic invariants and taking into account the large value of the plasma dielectric constant ($\varepsilon = 1 + nm/\varepsilon_0 B^2 = 10^3$–$10^5$), the equation of motion of the plasmoid can be integrated. The forward velocity in the Ox-direction is then given by:

$$v_x(x) = \left\{ v_{0x}^2 + 2\,\frac{\overline{\mu^+} + \overline{\mu^-}}{m}\,[B_0 - B(x)] \right\}^{1/2} \tag{3}$$

or by replacing $\bar{\mu}$, the average magnetic moments of the electrons and ions, by $kT_\perp/B$, Equation (3) becomes:

$$\tfrac{1}{2}mv_x^2 + kT_\perp^+ + kT_\perp^- = \tfrac{1}{2}mv_{0x}^2 + kT_{\perp 0}^+ + kT_{\perp 0}^- = \text{const.} \tag{4}$$

This implies that the sum of the translation and thermal energy densities of the ions and electrons is a constant of motion.

Note from Equation (3) that when the magnetic field intensity $B(x)$ is independent of x, as it is the case in Baker and Hammel's first series of experiments, the velocity $v_x(x)$ is also independent of x (see Figure 6). The validity of these equations has also been verified experimentally by Demidenko *et al.* (1966, 1967, 1969, 1972) for a non-uniform (but non-sheared) magnetic field distribution. A generalisation of these formulae for a sheared **B**-field has been given by Lemaire (1985).

4.2.6. *Penetration Across a Sheared Magnetic Field*

When the direction of the external magnetic field **B** rotates by an arbitrary angle θ across the magnetopause tangential discontinuity as illustrated in Figure 2, the vector **E** representing the electric field intensity inside the plasmoid, rotates by the same angle θ. Both vectors **E** and **B** remain orthogonal to each other according to Equation (2); $E(x)$ varies with x as $v_x(x)B(x)$ where $v_x(x)$ is given by Equation (3) (Lemaire, 1985).

Equation (3) can now be used to determine x_1 the maximum penetration depth of a plasmoid where $v_x(x_1) = 0$. Indeed, the value of the magnetic field intensity $B(x_1)$ is then determined by the value of the injection speed v_{0x} and of the mean magnetic moments $\bar{\mu}$ of the particles; note that $\bar{\mu}$ is determined by the perpendicular temperatures ($T^+_{\perp 0}$ and $T^-_{\perp 0}$) of the ions and electrons in the magnetosheath where the magnetic field intensity has the value B_0.

It can be verified that when realistic magnetosheath plasma temperatures $T^+_{\perp 0}$, bulk speeds v_{0x} and magnetic field intensity B_0 are used in Equation (3), the calculated magnetopause position compares well with the observed values (see Lemaire, 1985).

It should be pointed out that the total plasma pressure balance equation is generally solved to calculate the average position of the magnetopause. When the dynamical pressure term is taken into account the total pressure balance equation is given by

$$n(mv_x^2 + kT_\perp^+ + kT_\perp^-) + B^2/2\mu_0 = \text{const.} \tag{5}$$

The first term is predominant in the supersonic solar wind; while the last term is most important in the magnetosphere. This reasoning leads then to the following balance equation, provided the density inside the plasmoid is equal to the ambient solar wind density:

$$K(nmv_x^2)_{\text{solar wind}} = (B^2/2\mu_0)_{\text{magnetosphere}}, \tag{6}$$

where the constant factor K ranges between 1 and 2 to account for the 'non-specular' reflection of the solar wind against the magnetopause (Beard, 1960).

Note, however, that when the plasma density is larger than the background solar wind, Equation (5) gives a penetration depth which is larger than that obtained with Equation (6).

4.2.7. *Diamagnetic Signatures of Plasmoids at the Magnetopause*

Up to this point, the impulsive penetration mechanism has been discussed for the case of low-β, i.e., for plasmoids whose diamagnetic currents do not perturb significantly the external magnetic field distribution. On the contrary, when the value of β is of the order of unity, as it is often the case in the solar wind and magnetosheath, large diamagnetic effects perturb locally the external magnetic field intensity and direction. Magnetization currents circulate around (and possibly inside) the body of plasma irregularities. These currents are driven by gradients of kinetic pressure at the surface (or inside the volume) of these plasma clouds.

These currents are confined within or at the surface of the moving plasmoids; these currents are similar to the Chapman–Ferraro currents flowing around the magnetosphere. When a magnetometer onboard of a spacecraft approaches such a high-β diamagnetic current layer it measures a B-field variation, similar to those magnetic field signatures observed in the plasma boundary layer by ISEE 1 and 2 as well as by many other earlier satellites (Aubry *et al.*, 1970, 1971).

Figure 8 simulates for instance the magnetic field lines distribution when a cylindrical current system, like that of diamagnetic plasma elements, approaches the Earth's dipole. The magnetic field signatures that a magnetometer would measure across these diamagnetic plasmoids are similar to those measured by Russell and Elphic (1979) in their Flux Transfer Events (FTE). According to many authors these FTE's should be

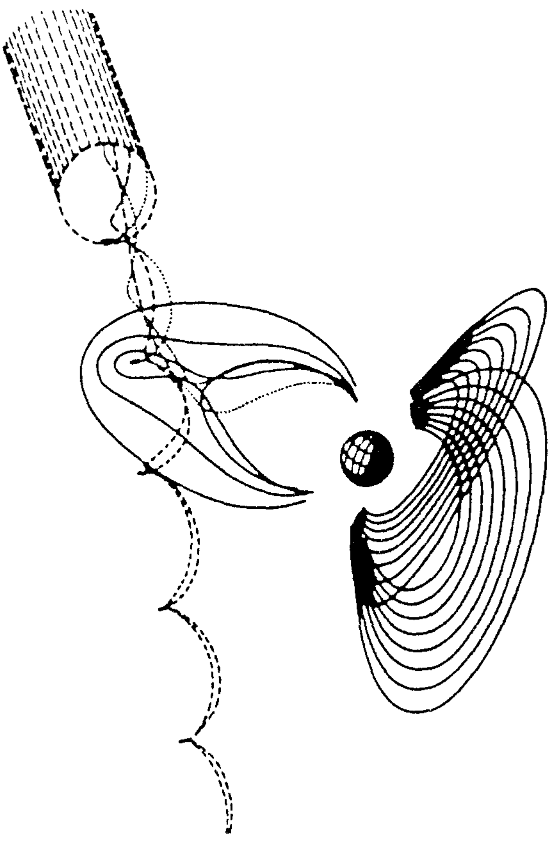

Fig. 8. Illustration of the perturbation of a dipole magnetic field produced by a filamentary current system. The magnetic field lines in the vicinity of the filament change shape when the diamagnetic plasmoid penetrates in the geomagnetic field. Some of the geomagnetic field lines become then interconnected with those of the interplanetary medium. This ressembles time dependent 'reconnection' or 'merging'. But this is simply the result of the superposition of non-stationary magnetic fields and does not involve anomalous resistivity nor any spontaneous and explosive plasma instability, as needed to produce FTEs.

the consequence of patchy and spontaneous explosive reconnection at the dayside magnetopause. Similar interpretations are also proposed by Lee and Fu (1985), Southwood (1987), Southwood *et al.* (1988), Scholer (1988), and Nishida (1989).

These MHD interpretations of FTEs imply a mechanism to initiate the postulated instability and to let it grow; *ad hoc* anomalous resistivity produced inside the volume element wherein the FTE originated, must be postulated; but it requires also an *ad hoc* nonlinear mechanism to quench this instability at a latter stage of its development, i.e., after a while the anomalous resistivity has to be set equal to zero to stop the growth rate of this instability.

For the previous authors the magnetic field signatures of Flux Transfer Events are not due to stable diamagnetic solar wind plasmoids injected from outside into the magnetopause region, but are 'events' produced by a local 'plasma' explosion: a kind of 'mini-flare' at the surface of the magnetopause where and when the IMF is antiparallel to the magnetospheric field. According to this interpretation these mini-explosive events occur spontaneously at the magnetopause: even when the impacting solar wind flow is uniform and stationary as in Figure 1(a). But no unanimously accepted description of the physical mechanism producing the anomalous resistivity and the resulting explosive events has yet been given.

There are many different types of magnetic field signatures observed during spacecraft crossing of the magnetopause, which are not similar to those particular ones identified as FTE; these other non-typical magnetopause crossings, (non-FTE) magnetopause signatures have not yet got buzzwords! This is probably the reason why nobody has yet been concerned about their nature nor about their origin. We consider that most of these B-field signatures (including FTEs) correspond to diamagnetic plasmoids of different shapes and of different origins, and brought by the solar wind to the place where they are observed. Therefore, according to our interpretation there is no need to postulate neither Kelvin–Helmholtz nor Rayleigh–Taylor instabilities, nor local anomalous effects in 'small diffusion regions' (as postulated in reconnection or merging theories) to explain most magnetic field observations near the magnetopause.

Note that we do not rule out completely such MHD instabilities, nor of course micro-instabilities in the Chapman–Ferraro current layers surrounding plasmoids or the magnetosphere itself. Indeed, when plasma density gradients are large, or when large velocity shears exist between the plasma inside and outside a plasmoid (or at the magnetopause) such instabilities can indeed occur as noticed by Roth (1978, 1979). The Rayleigh–Taylor instability could operate, on occasions when the solar wind flow impinging on the magnetopause is uniform and stationary. But what we have emphasized since the EGS meeting on the magnetopause regions (Amsterdam, 1976) where the liminaries of this theory were presented for the first time, is that one should not ignore nor overlook all small-scale plasma irregularities which are almost always present in the solar wind. Those which have an excess of momentum density can penetrate impulsively into the geomagnetic field. The entry of these plasmoids proceeds without having to postulate any kind of anomalous resistivity, and without having to trigger any explosive instabilities like those FTEs are assumed to result from.

4.2.8. *Induced Electric Fields*

When diamagnetic plasmoids approach the Earth magnetosphere they produce time dependent field variations in the geomagnetic field. If the value of β is large, large induced electric fields ($\mathbf{E}_i$) are generated by the time variations of the local magnetic field intensity $\dot{\mathbf{B}}$, or equivalently by time changes of the magnetic vector potential $\mathbf{A}$. This has been emphasized by Heikkila (1982, 1990). Indeed from Maxwell's equations

$$\partial \mathbf{B}/\partial t = -\nabla \wedge \mathbf{E}_i \,, \qquad \mathbf{E}_i = -\partial \mathbf{A}/\partial t \,, \tag{7}$$

it is obvious that local changes of the magnetic field like those observed in the solar wind and at the magnetopause necessarily generate induced electric fields whose intensities cannot be ignored in a self-consistent theory of the solar wind-magnetosphere interaction.

A simple order of magnitude calculation shows that magnetic field intensity variations of 2 nT measured over a period of 2 s (for instance across the surface of plasmoids moving past a stationary observer with a velocity of 400 km s^{-1}) will induce an electric field of 0.8 mV m^{-1}. Although, the convection electric field given by Equation (2) has a larger intensity (4 mV m^{-1}), it is clear that induced electric field cannot be ignored when β is large.

4.2.9. *Deformation of Geomagnetic Field Lines*

As a result of the local magnetic perturbations produced by moving diamagnetic plasma irregularities the distribution of magnetic field lines changes continuously with time, as illustrated in a video-film produced by the present authors in 1982 and available at the Institut d'Aéronomie Spatiale (Brussels). Figure 8 shows a picture taken from this simulation; it illustrates the deformations produced by a diamagnetic plasma filament interacting with a dipole magnetic field. The changing shape of interplanetary and geomagnetic field lines is illustrated, when this filamentary current system approaches the Earth dipole. The complex distributions of magnetic field lines are similar to those by Ogino *et al.* (1985, 1986).

Magnetic field lines passing through fixed points (forming a fixed grid) are drawn; these lines change shape when a diamagnetic plasmoid moves close-by. Except at the fixed grid points, all other parts of the field lines seem to 'move' when the highly diamagnetic plasma filament or cloud penetrates into the geomagnetic field. In our movie, this motion should not be confused, however, with what is commonly called 'magnetic field line motion'.

In the movie simulation there are points of the field lines which do not move ($\mathbf{v} = 0$), while other points along these same magnetic field lines change continuously position ($\mathbf{v} \neq 0$). Since in the MHD approximation magnetic field lines are equipotentials, the perpendicular electric field, $\mathbf{E} = -\mathbf{v} \wedge \mathbf{B}$, cannot be equal to zero at the fixed point without being zero at all other points along the field line. Therefore, the magnetic field lines deformations shown in this video-film should not be taken as an illustration of the ideal MHD concept of 'magnetic field lines motion'. Since there is no way to measure experimentally the 'velocity of a field line', we have abandoned this misleading paradigm.

In addition to small amplitude deformations of magnetic field lines the video-film shows also how geomagnetic field lines originally with both 'ends' rooted in the ionosphere, become 'open', i.e., interconnected with those of interplanetary space. Such interconnected magnetic field lines are shown in Figure 8. They have one 'foot' in the cusp ionosphere and the other one hangs in interplanetary space. These interconnected magnetic field lines ressemble those called 'reconnected' magnetic field lines by Dungey (1961). The bundle of field lines spiraling along the axis of the filamentary current system ressemble those which are drawn in cartoons representing FTE; they also ressemble those calculated by Farrugia *et al.* (1987) in their incompressible model of FTEs, or calculated by Ogino *et al.* (1985, 1986).

4.2.10. *Escape of Energetic Particles Out of the Magnetosphere*

Along the bundles of interconnected magnetic field lines energetic particles originally trapped in the magnetosphere can pipe out more easily into the magnetosheath and interplanetary medium.

Conversely, solar wind electrons and ions can spiral along these temporarily interconnected field lines into the Earth's magnetosphere (Lemaire, 1977).

Impulsively injected magnetosheath protons, alpha particles and electrons have indeed been observed by Carlson and Torbert (1980) in the cleft ionosphere. Their velocity dispersion indicates that they have been injected in a localized area of the frontside magnetopause at a well-defined instant of time. This place and this instant of time are those where and when the magnetic field lines passing through the point of observation become interconnected with those of the interplanetary space. The recent Viking results have been able to confirm this scenario (Lundin, 1988b).

Similarly, jets of escaping magnetospheric particles were observed first in the magnetosheath by Anderson *et al.* (1965). These energetic particles ($E < 25$ keV) are often present on magnetosheath lines near the magnetopause (Meng and Anderson, 1970, 1975; West and Buck, 1976; Daly *et al.*, 1979). Near the subsolar point they stream parallel or antiparallel to the magnetosheath magnetic lines in layers or jets outside the magnetopause (Korth *et al.*, 1979; Williams *et al.*, 1979). Energetic singly ionized helium and oxygen have been detected in these jets of escaping magnetospheric particles (Scholer *et al.*, 1981; Peterson *et al.*, 1982).

The interpretations of energetic particle observations at the magnetopause have generally been used to support the merging model (Scholer, 1983; Daly *et al.*, 1984). According to this interpretation magnetosphere particles escape into the magnetosheath along open (or interconnected) magnetic field lines that result from steady-state merging.

These interpretations are based on the assumptions that interconnected magnetic field lines represent the actual guiding center drift path of these energetic particles. However, in addition to their gradient-B and curvature drifts, these particles experience the electric drift velocity which is not specified by drawing a distribution of magnetic field lines. Furthermore, the distribution of these field lines is in general non-stationary due to constantly changing boundary conditions in the solar wind.

The guiding center of magnetospheric particles originally on a closed geomagnetic field line at $t = t_0$ can drift toward a magnetic field line which was open at starting time, t_0, without being able to escape because in the meanwhile, at $t = t_0 + \Delta t$ the magnetic field distribution has changed. The magnetic field line it is now spiraling around can again be closed.

This shows the limited usefulness of drawing stationary magnetic field line distributions in a constantly changing dynamical plasma boundary layer. Indeed, the true guiding centers of escaping particles are not determined by instantaneous cartoon representation of magnetic field lines. They follow complicated curves depending on the time-dependent magnetic and electric fields: $\mathbf{B}(x, y, z, t)$ and $\mathbf{E}(x, y, z, t)$.

This is why we consider with Sibeck *et al.* (1987) that drawing or calculating the actual drift path of energetic particles in the magnetopause region is much more adequate than just drawing magnetic field line distributions, as usually done. In this respect the 'leakage' model supported by Sibeck *et al*'s (1987) observations, describing the loss of magnetospheric particles by finite gyroradius effects is a much more realistic kinetic model than earlier MHD models which were proposed to explain the escape of energetic particles out of the Earth's magnetosphere.

Sibeck *et al.* (1987) show that although the merging model has often been used to explain individual sets of observations of the streaming ions, this MHD model is more limited than the leakage model originally introduced by Eastman and Frank (1982) and Papamastorakis *et al.* (1984), based on statistical studies. The merging process is of a limited extent, both spatially and temporally, while the 'leakage' model explain the almost continual escape of energetic particles observed for all magnetosheath magnetic field orientations. The merging model implies southward/IMF orientation exclusively.

4.2.11. *Eastward Deflection of Plasmoids Penetrating in the Geomagnetic Field*

The momentum density for a two-component neutral plasma is equal to

$$\rho = \rho \, \frac{\mathbf{E} \wedge \mathbf{B}}{B^2} - \frac{\rho}{Ze} \left[\frac{m^-}{2} \, (v_\perp^-)^2 \right] \frac{\mathbf{B} \wedge \nabla B}{B^3} - \\ - \frac{\rho}{Ze} \, [m^- (v_\parallel^-)^2] \, \frac{\mathbf{B} \wedge (\mathbf{B} \cdot \nabla)\mathbf{B}}{B^3} \, , \tag{8}$$

where ρ is the total mass density, $\mathbf{v}$ is the bulk speed of the plasma element, Ze is the electric charge of the ions and the brackets in these expressions are proportional to the perpendicular and parallel electron temperatures (Lemaire, 1985).

In the cold plasma approximation $T_\parallel^-$ and $T_\perp^-$ are both equal to zero, and, the total momentum density is only determined by the $\mathbf{E} \wedge \mathbf{B}/B^2$ drift velocity. However, when the plasma has a finite temperature the gradient-B and curvature drifts contribute to deflect the plasmoid in the $-\mathbf{B} \wedge \nabla B$ and $-\mathbf{B} \wedge (\mathbf{B} \cdot \nabla)\mathbf{B}$ directions, respectively. This corresponds to an eastward deflection of solar wind plasmoids penetrating impulsively into the magnetospheric plasma boundary layer, as illustrated in Figure 9.

It should be pointed out that the gradient-B and curvature terms depend on the ion mass to charge ratio. Therefore, the bulk velocity of different ion species in the plasma

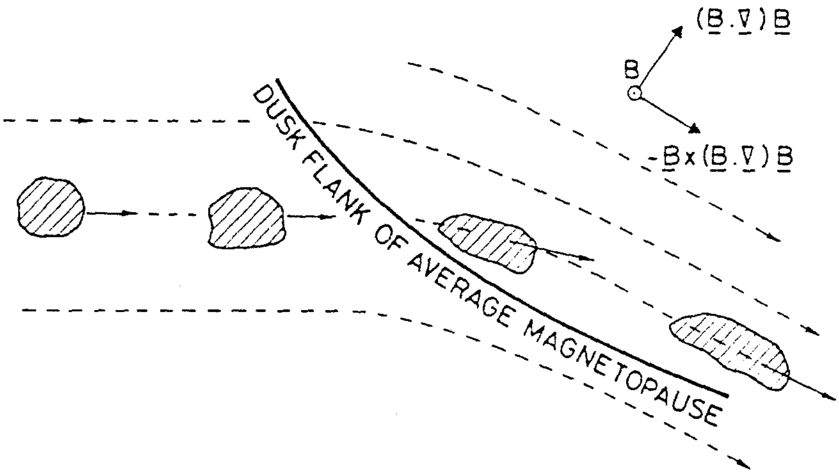

Fig. 9. Eastward deflection of solar wind plasmoids penetrating impulsively in the dusk flank of the magnetosphere. Both the grad-B and curvature drifts of the ions contribute to produce an eastward deflection of the intruding plasma irregularities (after Lemaire, 1985).

boundary layer will be different. This is precisely what has been observed by Lundin and Dubinin (1985) from Prognoz-7 observations. Within plasma density enhancements observed in the magnetopause region, the He^{++} ions (of solar wind origin) do not drift in the same direction as the He^+ and O^+ ions (of magnetospheric origin). They pointed out that in such multi-ion species plasmoids, the bulk velocity of the ions species can be significantly different from the $\mathbf{E} \wedge \mathbf{B}/B^2$ convection velocity which is the only drift considered in the 'ideal MHD' approximation.

Lundin and Dubinin's observations and Equation (8) clearly show that in a multi-ion species plasma whose electron and ion temperatures are not vanishingly small (hot plasma) the ideal MHD approximation breaks down. In this case the concept of magnetic field lines 'moving' with the $\mathbf{E} \wedge \mathbf{B}/B^2$ velocity is obsolete. Indeed, 'the motion of field lines' does not determine anymore (as it could do for zero temperature plasma) where the electrons and all the different ions species drift as a whole. Each ion species has its own drift path which is a consequence of gradient-B, curvature drifts and also polarisation drifts. A multicomponent plasmoid with a finite temperature does not follow the same drift path than an ideal MHD plasma irregularity.

Furthermore, inside the plasmoid itself the ions of different species may have different internal motions depending on their mass over charge ratio. In addition to the center of mass motion mainly considered above, the plasma inside a plasmoid can have internal motions: rotational and eddy convection motions with non-zero helicity is most likely possible to appear (as illustrated in Figure 7). The well-known two-cells convection pattern existing in the magnetosphere (considered here as a huge plasmoid moving in the solar wind with a supersonic speed) is a typical example of plasma circulation that can be expected in small scale plasmoids as well (see Schindler, 1979). But the study of plasmoids with non-zero helicity is far beyond our current concern. One would need very high-resolution plasma observations and an armada of four or more cluster-type spacecraft. Nevertheless, it is an interesting hydromagnetic problem to be studied in the future.

4.2.12. *The Influence of IMF B_z on Impulsive Penetration*

Plasmoids with an excess momentum which are moving with the background solar wind bulk velocity, have an excess mass density. Assuming nearly equal perpendicular plasma temperatures inside and outside the plasma irregulrity, it can be inferred that the perpendicular pressure ($nkT_\perp^+ + nkT_\perp^-$) is then larger inside than outside the element of plasma. As a matter of consequence the magnetic energy density ($B^2/2\mu_0$) must be smaller inside than outside in order to satisfy pressure balance equilibrium. The magnetic dipole moment (**M**) of the diamagnetic currents circulating in the plasmoid as well as on its surface, is then pointing in a direction opposite to the ambient interplanetary magnetic field **B** (Lemaire *et al.*, 1979).

When the IMF has a northward component (i.e., $B_z > 0$), the magnetic dipole moment **M** of a diamagnetic plasmoid with an excess density has a southward component (i.e., $M_z < 0$). It can be shown that the magnetic force, $\nabla(\mathbf{M} \cdot \mathbf{B}_E)$ exerted on a southward oriented magnetic dipole moment **M** by the geomagnetic field, $\mathbf{B}_E$, which has a southward oriented dipole component, $\mathbf{M}_E$, is directed away from the Earth. When such a plasmoid is at low latitudes near the frontside magnetopause, **M** being there nearly parallel to $\mathbf{M}_E$, both dipoles repel each other. In other words, the diamagnetic current loops producing the magnetic field depression inside the plasmoid are then pushed away by the southward oriented Earth's dipole $\mathbf{M}_E$. The dipole-dipole interaction acts then to reject the intruding small-scale plasma current system out of the geomagnetic field distribution, or at least to decrease its entry velocity in the low-latitude boundary layer.

Above the northern and southern magnetotail lobes the IMF field lines are draped along the magnetopause surface. When in front of the bow shock the IMF B_z is positive, the directions of magnetic field lines in the magnetosheath are titled in the anti-sunward (sunward) direction above the northern (southern) magnetotail surface. A plasmoid with an excess momentum density and an excess thermal pressure necessarily has a magnetic moment pointing in a direction opposite to **B** in the magnetosheath, i.e.:

$M_x > 0$ above the northern magnetopause where $B_x < 0$.

$M_x < 0$ above the southern magnetopause where $B_x > 0$. The magnetic force, $\nabla(\mathbf{M} \cdot \mathbf{B}_E)$, acting on the dipole moment **M** is directed toward the interior of the magnetotail over the magnetopause area located beyond the polar cusp.

In other words, solar wind irregularities with an excess density are attracted toward the inside of both magnetotail lobes when the IMF is northward. On the contrary, for a southward IMF, the dipole-dipole interaction between plasmoids and the geomagnetic field favors impulsive penetration in the frontside magnetosphere, but not in the magnetotail lobes.

The same conclusions have already been reached in a previous article by Lemaire *et al.* (1979). Unfortunately, the captions of Figures 6 and 8 in this article are interchanged. Moreover, it contains on pages 50 and 51 incorrect statements concerning the force acting between current systems. In this article, only 2-D plasma current sheaths were considered (tangential discontinuities). However, the actual surface of plasmoids is a 3-D surface. The surface currents have a finite magnetic moment as illustrated in Figure 10; this is not the case for 2-D flat current systems interacting on each other.

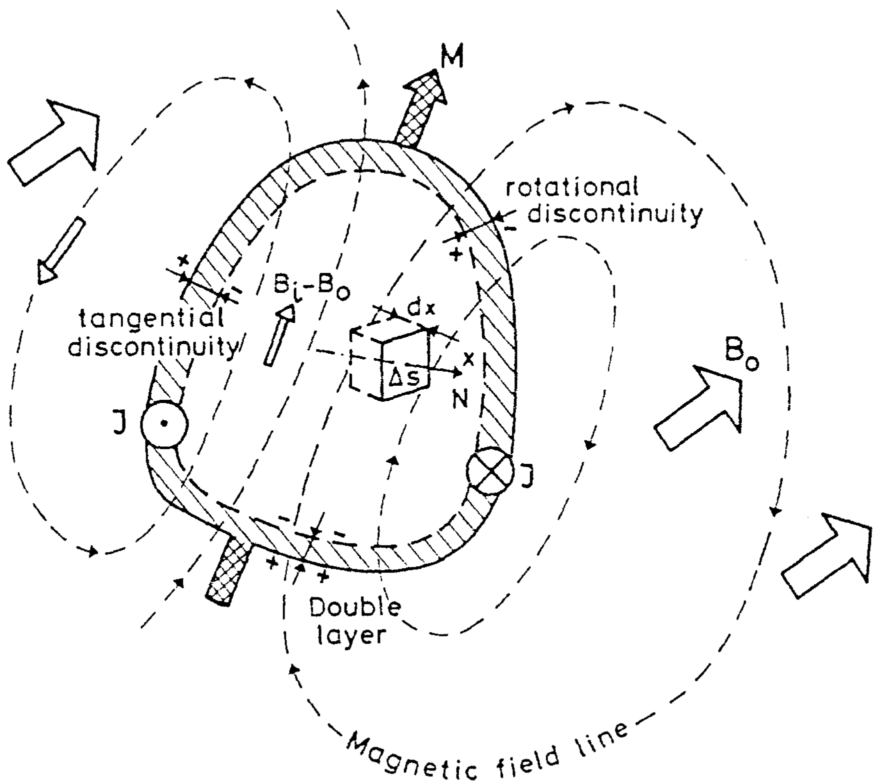

Fig. 10. The hatched area is the cross section of the current layer surrounding a diamagnetic plasmoid engulfed in an external magnetic field $\mathbf{B}_0$. The magnetization currents **J** reduce the magnetic field intensity inside the plasma density enhancement. **M** is the dipole magnetic moment of this electric current system. The magnetic field lines produced by this current layer are shown by dashed lines. Where they traverse the surface of the plasmoid, one has a rotational discontinuity; where the field lines are tangent, the surface is a tangential discontinuity. In both cases electrostatic double layers appear at the surface of the plasma density enhancement.

Therefore, a dipole-dipole interaction force like that discussed above does exist only in the case of 3-D objects, but not for flat 2-D dimensional current sheaths of infinite extent. When these 2-D planar current sheaths (with zero magnetic dipole moment) are indeed replaced by 3-D plasmoid (with non-zero magnetic dipole moment), the conclusions in the paper by Lemaire *et al.* (1979) are applicable: i.e., impulsive penetration of plasmoids with an excess kinetic pressure is favoured in the magnetotail lobes when the IMF B_z is positive. The physical reason for this effect is the dipole-dipole interaction force between the Earth's dipole and the magnetic dipole moment of the 3-D solar wind plasmoids.

4.2.13. *The Influence of IMF B_y on Impulsive Penetration*

The dipole-dipole force acting on a diamagnetic magnetosheath plasmoid is maximum in the vicinity of the polar cusps where the spatial derivatives of $(\mathbf{B}_E)_x$, $(\mathbf{B}_E)_y$, and $(\mathbf{B}_E)_z$ are largest. For any IMF direction and any orientation of **M**, there is always a location in the vicinity of the neutral points where the magnetic field direction in the magnetosheath is antiparallel to the magnetospheric field. This is where the magnetic force $\nabla(\mathbf{M} \cdot \mathbf{B}_E)$ is maximum and directed toward the interior of the magnetosphere. When IMF $B_y > 0$ this place is shifted toward dusk (dawn) with respect to the location of the northern (southern) polar cusp. As a consequence, the region of preferred impulsive penetration of solar wind plasmoids is shifted toward dusk (dawn) in the northern (southern) hemisphere as illustrated in Figure 11. The direction of these shifts is reversed in both hemispheres when IMF $By < 0$.

4.2.14. *Magnetospheric and Ionospheric Convection Patterns Resulting from Impulsive Penetration in the Magnetotail*

When a solar wind plasma density irregularity is injected in the magnetotail as illustrated in Figures 11(b) and 12(a), the ambiant magnetospheric plasma is pushed aside and flows along the flanks of the intruding plasma body. Figure 12(a) represents a cross section through the northern magnetotail. The reader is looking toward the direction of the Sun.

The direction of the bulk velocity vectors in the surrounding magnetospheric plasma is opposite to the velocity of impact for the solar wind plasma irregularity. This necessarily leads to a transient flow pattern of magnetospheric plasma in the tail lobes. This transient flow pattern is illustrated in Figures 11(b) and 12(a) by small arrows directed toward the surface of the magnetosphere away from the center of the magnetotail.

The convection electric field, **E**, associated with this transient flow of magnetospheric plasma across geomagnetic field lines is indicated by open arrows in Figure 12(a). Outside the plasma element, the surface charges produce a dipolar E-field perturbation. Since the magnetospheric **B**-field is pointing toward the Sun in the northern tail lobe, the electric field, $\mathbf{E} = -\mathbf{v} \wedge \mathbf{B}$, outside the plasma element is oriented from dusk to dawn. This convection electric field maps down into the polar cap ionosphere as illustrated in Figure 12(b). Note that the convection electric field inside the intruding plasmoid does not map into the ionosphere when the magnetic field lines traversing this plasma element are not connected to the polar cap. When they become interconnected, a field-aligned electric potential drop appears, where these field lines penetrate through the surface of the plasmoid. The dusk-dawn electric field drags ionospheric plasma over the polar cap in the direction of the Sun as indicated in Figure 12(b) by the arrows pointing toward 12:00 LT.

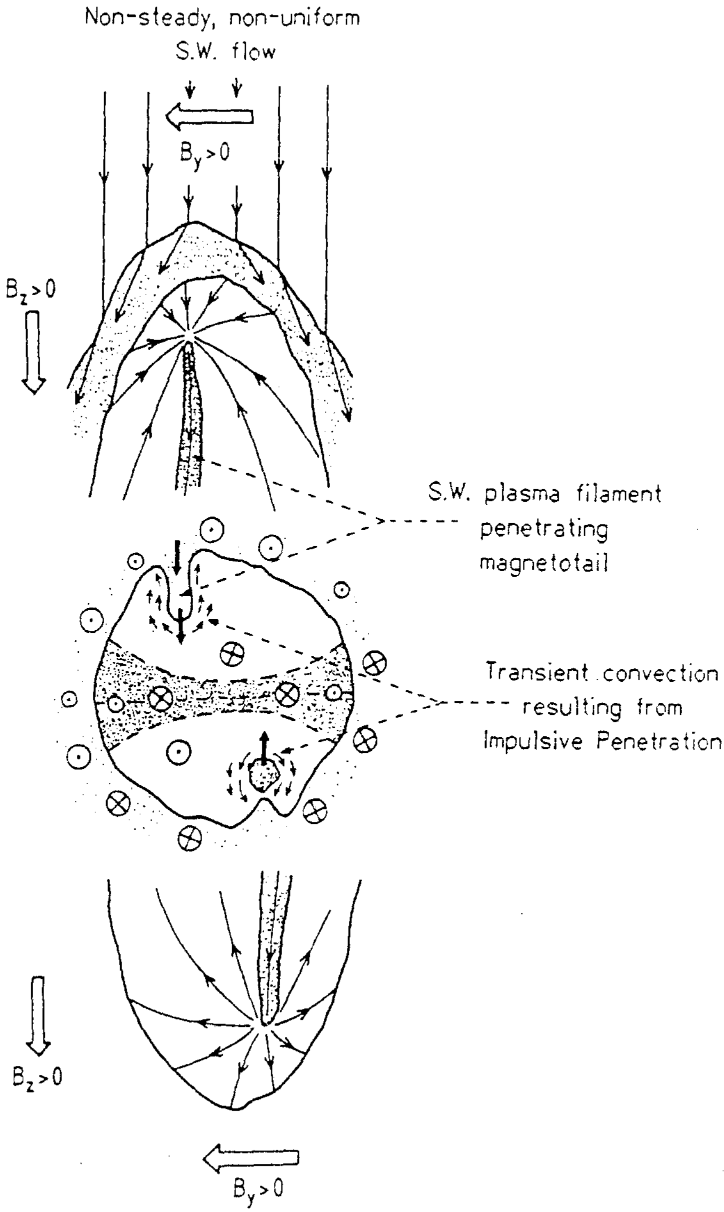

Fig. 11. Cartoons illustrating the bumpy shape of the magnetosphere in a non-steady and non-uniform solar wind plasma filament penetrating across the surface of the northern magnetotail lobe when the IMF has a northward B_z (NBZ) component. The neutral point of the northern polar cusp is shifted toward dusk when the IMF B_y component is positive. The bottom panel corresponds to the penetration of a solar wind plasmoid in the southern tail lobe for the same IMF condition. Note that the southern polar cusp is shifted toward dawn. The central panel represents a cross section of the magnetospheric tail lobes and of the plasmasheet (dotted area). The transient flow of magnetospheric plasma around impulsively injected solar wind plasmoids is illustrated by small arrows. The observer is facing the Sun in the central panel (after Lemaire, 1987).

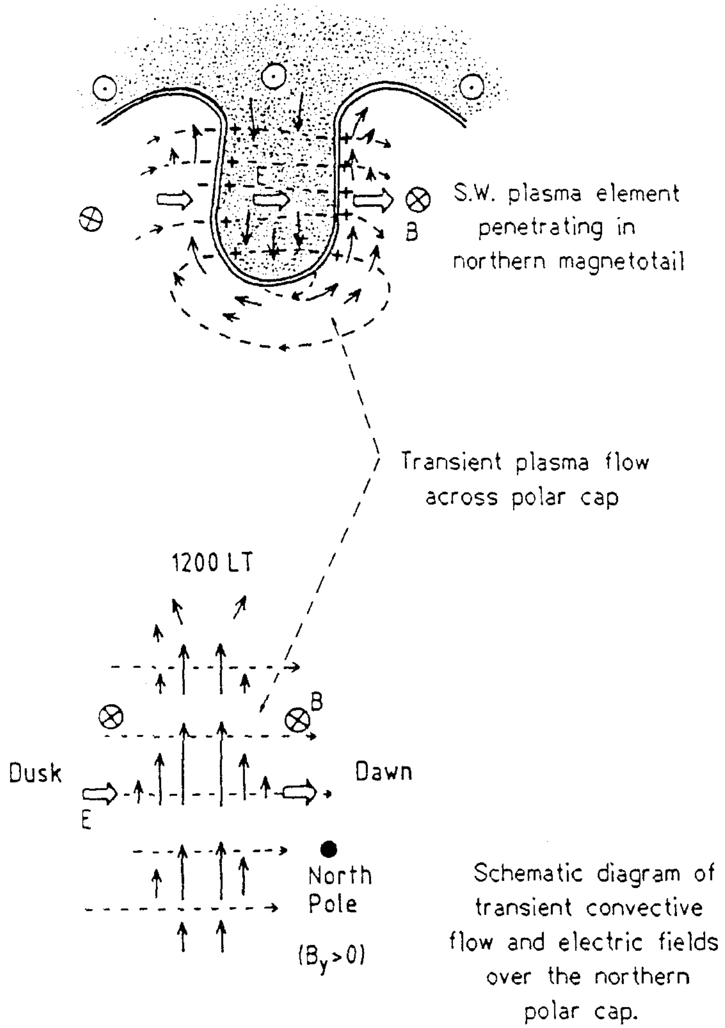

Fig. 12. Transient flow pattern around a solar wind plasma element penetrating impulsively in the northern magnetotail lobe. The observer is facing the Sun in the top panel. The dusk-to-dawn convection electric field is displayed, as well as electric field lines (dashed lines). The bottom panel illustrates the convection electric field and sunward plasma flow patterns at ionospheric heights over the northern polar cap when IMF $B_z > 0$ and IMF $B_y > 0$ (after Lemaire, 1987).

Sporadic sunward flow of ionospheric plasma over the northern and southern polar caps has indeed been observed when the IMF has a northward B_z component. Sunward flow in the polar cap ionosphere was first presented by Maezawa (1976) and substantiated by data by Burke *et al.* (1979) and by Zanetti *et al.* (1984). The locations where sunward flows were observed are shifted toward the dawn or dusk side of the polar caps depending on the sign of IMF B_y. The directions of these observed shifts correspond precisely to those of the preferred region of penetration of solar wind plasma irregularities into the magnetotail lobes, when IMF $B_z > 0$ and IMF $B_y > 0$.

The non-stationary flow patterns shown in Figures 12(a) and 12(b) can of course be superimposed on the stationary convection flow patterns inferred from steady-state interaction models like those proposed by Crooker (1979), Reiff (1982), Reiff and Burch (1985), Lyons *et al.* (1985), or Kan and Burke (1985). Note, however, that a large number of small-scale solar wind plasma elements penetrating continuously through a wide area of the tail lobes can drive a large-scale quasi-stationary sunward convection flow pattern over a wide area of the polar caps. A large ensemble of small-scale plasmoids can produce an average large-scale sunward convection flow similar to that described in the steady-state anti-parallel merging models mentioned above. Like for the large number of droplets forming a rain shower and pouring into surface water, the large number of plasma density irregularities forming a disturbed solar wind flow can penetrate in the magnetotail and change the global convection in the plasma mantle as well as in the coupled ionosphere. This continuous entry of plasmoids over a broad portion of the magnetotail surface drives a global convection flow over a much wider volume of the magnetosphere than just one single small-scale plasmoid. It drives also an average large-scale sunward convection over a broad portion of the polar cap ionosphere. Each individual plasma 'droplet' contributes locally to the overal stream. The duration of time, as well as the area of the polar cap ionosphere influenced by impulsive penetration of magnetosheath small irregularities do not depend so much on the size of these individual irregularities, than on the width and length of the solar wind volume where the plasma is turbulent and patchy. When the solar wind is non-uniform and patchy over heliocentric radial distances larger than 35 000 000 km, the shower of plasmoids penetrating in the magnetosphere will last longer than one day. In these circumstances a quasi-stationary convection flow pattern has time enough to build up in the magnetosphere and in the ionosphere. But a true stationary regime can be established only when the small-scale plasma irregularities are evenly distributed within the solar wind volume, and, when the IMF B_z keeps a fixed orientation for long enough time.

4.2.15. *Ionospheric Convection Patterns Resulting from Impulsive Penetration in the Frontside Magnetosphere*

During periods of prolonged southward IMF, the direction of the global convection flow is anti-sunward over the polar caps (Heppner, 1972). When the interplanetary magnetic field has not a northward component, the penetration in the magnetotail lobes is not favored. In this case, the frontside magnetopause is the most favorable place for solar wind irregularities to penetrate impulsively (Lemaire *et al.*, 1979).

Lemaire (1977, 1979b, 1987) argued that the anti-sunward flow over the polar cap is then a consequence of continuous impulsive penetration of solar wind plasmoids in the frontside magnetosphere when IMF $B_z < 0$.

Goertz *et al.* (1985) and Sandholt *et al.* (1986) have observed transient poleward motions of small-scale structures in the dayside auroral ionosphere during periods of southward IMF. We associate these with impulsive penetration of solar wind plasma density irregularities into the dayside plasma boundary layer when the IMF B_z is negative. Indeed, when such blobs of plasma intrude into the magnetosphere, the ambient magnetospheric plasma is pushed aside and flows along the flanks of the penetrating solar wind plasma density enhancements. The directions of bulk velocity vectors for the surrounding magnetospheric plasma is opposite to the velocity of impact of the plasmoid. As already described in Section 4.2.14, this is a consequence of the dipole electric field generated outside the penetrating plasmoids by the electric charges at its surface. This leads to a transient flow pattern which maps into the ionosphere on the equatorward side of the polar cusps, i.e., in the region called 'boundary cusp' illustrated in Figure 13 (after Kremser and Lundin, 1988). The corresponding transient ionospheric convection is indeed poleward as observed by Goertz *et al.* (1985) and Sandholt *et al.* (1986).

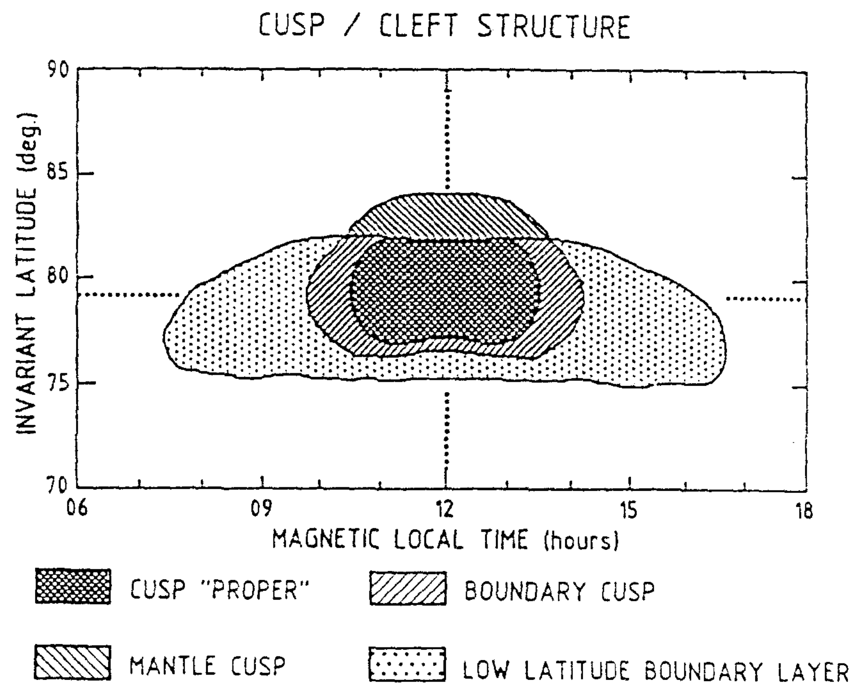

Fig. 13. Summary plot of the polar cusp and cleft from a statistical study using Viking particle data (from Kremser and Lundin, 1988). Four different regions are distinguished: – The cusp 'proper' characterized by high fluxes of isotropic magnetosheath electrons and ions with no signatures of particle acceleration. – The 'active' boundary cusp with lower magnetosheath plasma densities and moderate acceleration of electrons and ions. – The mantle cusp, i.e., the region with tailward flowing ions connected to the plasma mantle. – The dayside auroral region connected to the low latitude boundary layer. This region is characterized by time-dependent magnetosheath plasma injection and strong plasma acceleration.

More recently Todd *et al.* (1986) using radar data, Lanzerotti *et al.* (1986, 1987), Friis-Christensen *et al.* (1988), and Heikkila *et al.* (1989) using correlated ground based and satellite observations, have been able to show that the convection patterns induced into the 'boundary cusps' (as defined in Figure 13) by impulsively injected solar wind plasma irregularities, form westward propagating double vortex structures. The distribution of the convection velocities in these twin vortices is illustrated in Figure 14, taken from Friis-Christensen *et al.* (1988). This corresponds to poleward flow of about 1 km s^{-1} between two field-aligned currents and weaker return flows on both sides. This whole pattern observed in the prenoon local time sector moved to the left (i.e., westward, tailward) with high speeds, 3–6 km s^{-1}. Heikkila *et al.* (1989) emphasize that the poleward plasma convection between the two vortices does not indicate poleward motion of the whole disturbance. As already indicated above, similar disturbance observed closer to noon magnetic local time meridian should propagate equatorward, while those occurring in the post-noon local time sector should tend to move eastward (i.e., also tailward).

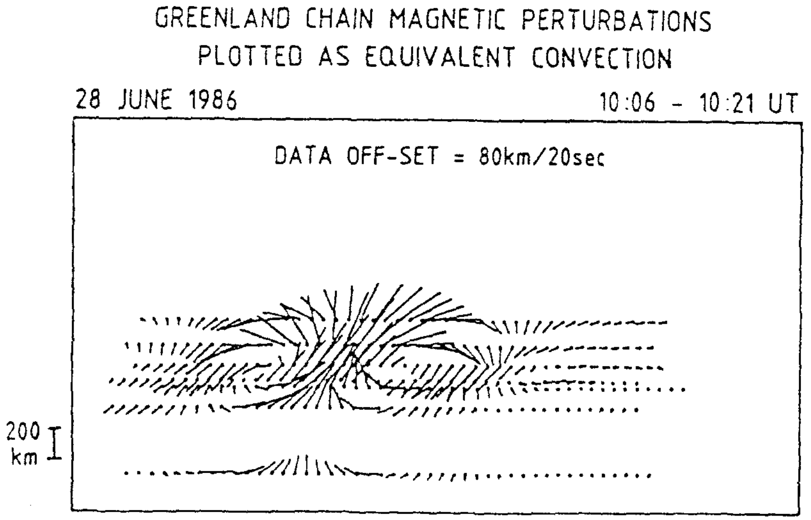

Fig. 14. The convection pattern that can reproduce the observations of Friis-Christensen *et al.* (1988). It is a double vortex, with poleward flow of about 1 km s^{-1} between the two field-aligned currents and a weaker equatorward return flow. This whole pattern moved to the left (westward and tailward) with very high speeds, 3 to 6 km s^{-1} (from Heikkila *et al.*, 1989).

Heikkila *et al.* (1989) explain the formation of these twin vortices by the mechanism of impulsive penetration of solar wind plasma through the magnetopause into closed magnetic field lines. Heikkila's *et al.* (1989) representation of the impulsive penetration event through the magnetopause is sketched in Figure 15(b).

The effects of a localized burst of reconnection at the magnetopause as sketched by Southwood (1987) is given in Figure 15(a) for comparison. After such an explosive reconnection event spontaneously generated the reconnected flux tubes (north as well as south) map to the equatorward edge of open magnetic field lines in the polar caps. According to this interpretation these reconnected flux tubes would correspond to an equatorward bulge in the boundary between open and closed field lines.

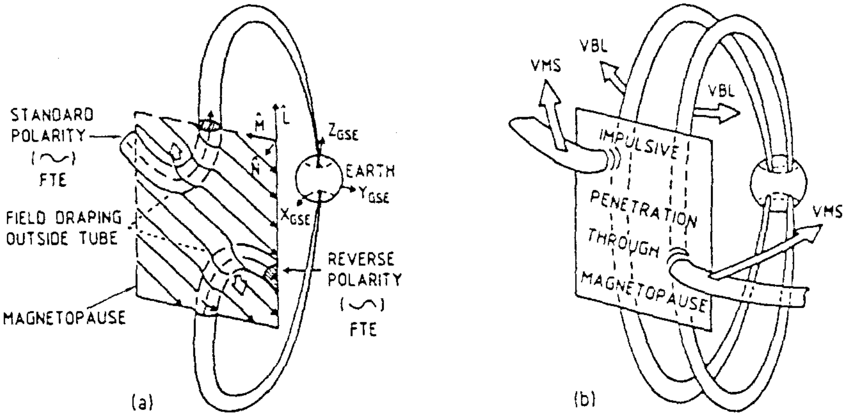

Fig. 15. (a) A sketch illustrating the effects of a localized burst of reconnection at the magnetopause (after Southwood, 1987). In the subsequent motion, the reconnected tubes (north as well as south) map to the equatorward edge of open field lines in the polar caps, corresponding to an equatorward bulge in the boundary between open and closed field lines. (b) Heikkila *et al.* (1989) representation of an impulsive penetration event through the magnetopause into closed field lines. Such a mechanism leads to two separate disturbances on closed field lines, on the morning side as well as on the afternoon side. In both sketches, it is implicitly assumed that the volume of the plasma entity (or plasmoid) coincides precisely with a whole magnetic flux tube (From Heikkila *et al.*, 1989).

In both sketches of Figure 15 it is implicitly assumed that the volume of the plasma entity (or plasmoid) coincides precisely with a whole magnetic flux tube: i.e., that the plasma has very rapidly filled up the whole volume of the flux tube. But this assumption is another reminiscence of the ideal MHD paradigm. Indeed, from the laboratory experiments of Bostick (1957) and Demidenko *et al.* (1969), it can be seen that a plasma-field entity (i.e., a plasmoid) does not necessarily fill a whole magnetic flux tube within the vacuum chamber.

Although a field-aligned filamentary shape is usually postulated for ‘obvious reasons’, we wish to point out here that field-aligned electrostatic double layers (always overlooked in the ideal MHD approximation of plasma physics) and associated field-aligned pressure gradients can easily prevent a plasmoid from spreading rapidly along external magnetic flux tubes (Lemaire and Scherer, 1978). Therefore, instead of postulating that the volume of the ‘reconnected’ flux tube (Figure 15(a)) or the ‘disconnected’ magnetic flux tube (Figure 15(b)) are almost instantaneously filled up with magnetosheath-like plasma, we are used to picture the penetrating plasmoid as a compact 3-dimensional structure (i.e., a plasma-field entity) which does not necessarily stretch out along the direction of the magnetic flux tubes.

The dimensions and shape of this plasma cloud are the result of all mechanical deformations it has experienced in the solar wind, during its passage through the bow shock, and during its impulsive entry into the geomagnetic field. This is why we choose to represent in Figure 16 the plasmoid as a nearly-spherical plasma entity, instead of as the volume of a ‘magnetic flux tube’.

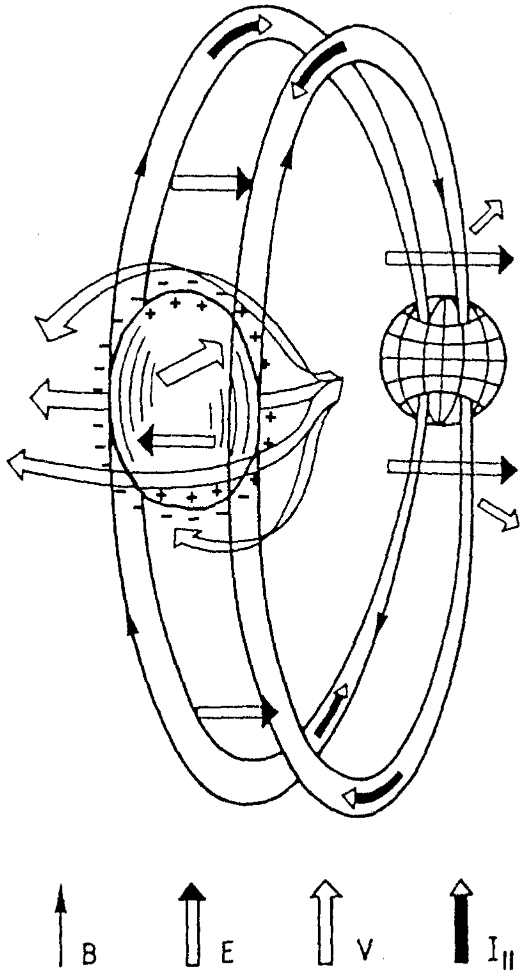

Fig. 16. Three-dimensional structure of a penetrating plasmoid. The latter is a nearly spherical plasma entity instead of the volume of a magnetic flux tube. The double vortex structure given in Figure 14 and the associated current systems found by Friis-Christensen *et al.* (1988) can be explained within the framework of this three-dimensional illustration of a plasma cloud.

It can be shown that the observed double vortex structure given in Figure 14 and the associated current systems found by Friis-Christensen *et al.* (1988), can simply be explained within the framework of the alternative mechanism illustrated in Figure 16. This 3-dimensional illustration of a plasma cloud of finite extent in all directions, drifting earthward across closed geomagnetic field lines, is a more realistic representation of what was called originally the 'theory of impulsive penetration'.

4.2.16. *Erosion of Plasmoids*

The basic kinetic description of the physical mechanism setting up the polarization electric field within a plasmoid, and permitting it to conserve its momentum while it penetrates in a higher magnetic field, was first outlined by Schmidt (1960) and Dolique (1963a, b). See also some plasma physics textbooks like that of Fälthammar (1973, p. 133) or Schmidt (1966). This kinetic theory has been applied by Demidenko *et al.* (1969) to explain the adiabatic deceleration and acceleration of the plasmoids in their laboratory experiments. It has been extended for the case of sheared magnetic field distributions by Lemaire (1985).

It has been pointed out by Heikkila (1982) that there is a limit in the ability of the polarization currents (due to the inertial drifts of the ions and electrons, due to the gradient-B drifts and curvature drifts of these particles) to deliver charges to the flanks of the plasmoid. Particles drifting aside into the surface layer experience a smaller electric field than the bulk of the plasma deep in the moving plasma cloud. As a matter of consequence, they are left behind and maintain an extra polarization **E**-field in the wake of the intruding plasmoid. This extra polarization electric field produced by the ions and electrons eroded from the flanks of the plasma entity should drag magnetospheric plasma in the wake behind it.

Since the electric field intensity within the plasma is maintained such that E/B is constant (or varies to conserve momentum), the electrons and ions lost from the surface layer are continuously replaced from the plasma interior. Thus the plasma cloud velocity remains unchanged, while its mass gradually decreases, as a result of the possible erosion effect. Heikkila *et al.* (1989) believe that, eventually, the plasma cloud runs out of steam before it is stopped by the adiabatic and non-adiabatic deceleration processes discussed in Sections 4.2.4 and 4.2.3. This can well be the case for plasma clouds of small mass. But for larger solar wind plasma irregularities the adiabatic and non-adiabatic braking (deceleration) processes will have converted its excess kinetic energy into gyro-motion before the whole mass has been eroded by the mechanism mentioned by Heikkila (1982) and also discussed by Dolique (1963a, b) for laboratory plasma streams penetrating into a non-uniform magnetic field.

Like many other effects qualitatively described in the space plasma literature, this erosion effect needs a more quantitative description than now available. Indeed, the ability to erode charges from the surface layer of a plasmoid must depend on a number of plasma and B-field parameters (e.g., the electron and ion gyro-radii, the value of the plasma 'beta', and the Debye length). The influence of these physical parameters on the rate of erosion needs to be simulated and worked out on a more quantitative basis.

4.2.17. *Mass- and Momentum-Loading Effects*

There is another effect that influences the motion and deceleration of plasmoid ions impulsively injected into the Earth's magnetosphere: it is momentum exchange of magnetosheath ions with the ambient magnetospheric ions. This effect is also called mass loading of a plasma stream. A region where the injected (magnetosheath) ions drift with a different bulk velocity than the ambient (magnetospheric) ones is considered in engineering plasma textbooks as a 'dynamo under load'. In such localized plasma regions the average drift velocities of the different ions species differ between each others. They differ also from the classical convection electric drift: $\mathbf{V}_E = \mathbf{E} \wedge \mathbf{B}/B^2$. A dynamo loading parameter, K, is then defined for each ion species as the ratio between the convection electric velocity V_E, and the measured average ion drift velocity $\langle v_i \rangle$, $K = V_E/\langle v_i \rangle = E/\langle v_i \rangle B$. An efficient dynamo is generally characterized by a loading parameter $K \approx 0.5$ (Lundin, 1988a).

Evidence for mass loading and differences between the average velocity of the injected magnetosheath ions (He^{++}) and the 'cold' local He^+ and O^+ ions which are both present in plasma density enhancements observed in the low-latitude boundary layer, was found by Lundin (1984), Lundin and Dubinin (1985), Lundin *et al.* (1987) using PROGNOZ-7 ion-composition measurements. These detailed and important observations confirmed that the injected solar wind ions have initially an excess momentum compared to the ambient (pre-existing) ions which poured into the intruding plasma element along the magnetic field lines traversing its 3-dimensional surface.

The local momentum exchange between the pre-existing boundary layer plasma and the injected plasmoid was first studied by Lundin and Dubinin (1985). A more detailed description of the macroscopic ion flow in the boundary layer, based on the first-order drift theory, has been given by Lundin *et al.* (1987). They showed that the relative difference ($\mathbf{R}_i$) between the drift velocities of the injected ($\langle \mathbf{v}_i \rangle_i$) and the ambient ions ($\langle \mathbf{v}_i \rangle_{\mathrm{terr}}$) defined by

$$\mathbf{R}_i = (\langle \mathbf{v}_i \rangle_i - \langle \mathbf{v}_i \rangle_{\mathrm{terr}}) \wedge \mathbf{B}/\langle \mathbf{v}_i \rangle_i \wedge \mathbf{B}\,, \tag{9}$$

is inversely proportional to the ratio $R_n = (n_i + n_{\mathrm{terr}})/n_i$, where n_i and n_{terr} are, respectively, the injected ion density and the density of the ambient ions which are of terrestrial (plasmaspheric) origin.

The ion composition measurements by Lundin *et al.* (1987) clearly confirmed that $R_i \sim 1/R_n$ for $R_n \gg 1$. This indicates that the higher the ambient magnetospheric plasma density is (R_n large) the smaller the difference between the bulk speed of the different ion species, due to the more efficient momentum exchange between both particle species (R_i is then small). This case corresponds to a dynamo with a strong internal load and by consequence, large depolarization currents (see Lundin, 1988a). In the case of high internal load the ambient plasma takes up quickly the momentum of the injected plasma of solar wind origin.

For plasmoids with small magnetosheath densities ($R_n \approx 1$), the ambient magnetospheric ions behave as test particles and the difference in average ion drift velocities is large. It reflects the characteristics of a dynamo under external load only. The ionosphere is part of the external load which slows down the bulk speed of the intruding plasma element as explained in Section 4.2.3.

Lundin (1988a) notices also that these ion composition measurements clearly demonstrate that the ideal MHD approximation of plasma physics is not applicable inside the plasma density enhancements observed by PROGNOZ-7, since all ion species do not drift with the so-called 'velocity of magnetic field lines': $\mathbf{v}_E = \mathbf{E} \wedge \mathbf{B}/B^2$.

Lundin *et al.* (1987) also found from PROGNOZ-7 observations that the differences between the drift velocities of the various types of ions tend to vanish deeper in the boundary layer region. This confirms nicely Lundin and Dubinin's (1985) momentum and mass loading theory. Indeed the deeper the injected ions have penetrated into the magnetosphere the more time they have had to transfer their momentum to the ambient cold ions. Therefore, R_i must be smaller at the inner edge of the magnetospheric boundary layer than close to its outer edge.

Another finding deduced from PROGNOZ-7 ion-composition measurements by Lundin and Dubinin (1985), is that once the cold ambient ions have gained the same drift velocity as the injected ones, their translational energy is converted adiabatically into perpendicular thermal energy (gyro-energy) when the mass loaded plasmoid proceeds inwards and is eventually stopped as described in the Sections 4.2.3 and 4.2.4. Lundin (1988a) showed that these experimental observations support the theoretical results given by Equation (4).

It should finally be pointed out that the magnetospheric ions do not penetrate inside the intruding plasmoid by anomalous diffusion across magnetic field lines tangential to its surface. As discussed in Section 4.2.14 we consider that the magnetospheric ions are slipping along these portions of the surface, like the magnetosheath plasma slips along the surface of the magnetosphere.

The easiest way for these ambient ions to move inside the plasma element is along the magnetic field lines which traverse its surface. The portions of the plasmoid surface crossed by these field lines are rotational discontinuities or oblique electrostatic double layers. Magnetospheric ions must have sufficient energy to overcome the small electrostatic potential existing in the double-layer region surrounding the plasmoid as a result of the charge separation between its ions and electrons. The corresponding electrostatic potential energy is not much larger than the thermal energy of the most dominant electron population (i.e., < 1 eV for plasmaspheric electrons, less than 20 eV for magnetosheath electrons, or 30 keV for trapped magnetospheric electrons). Therefore, depending on the thermal energies of the particles interacting at the surface of the plasmoid, only ions above a given energy can penetrate inside the volume of the drifting element.

The mass loading through the oblique double layer at the edge of the plasma element does not imply any kind of anomalous resistivity, nor any kind of spontaneous reconnection events triggered by an *ad hoc* plasma instability. It is a simple consequence of a plain kinetic description of the impulsive penetration process.

5. Observational Support for the IP Scenario

After the observations by the ATS1 (Freeman *et al.*, 1968) and VELA (Hones *et al.*, 1972; Akasofu *et al.*, 1973) satellites indicating the presence of magnetosheath plasma immediately inside the flanks of the magnetotail, data obtained by HEOS-2 (Haerendel *et al.*, 1978), EXPLORER 33 (Crooker, 1977) and IMP 6 (Eastman *et al.*, 1976) demonstrated the existence of a similar boundary layer near the polar cusps and inside the low-latitude portion of the magnetopause.

Four different boundary layers were recognized: the low-latitude boundary layer (Eastman *et al.*, 1976, Eastman and Hones, 1979); the plasma mantle (Rosenbauer *et al.*, 1975), the entry layer (Paschmann *et al.*, 1976), and the exterior cusps (Hansen *et al.*, 1976; Schopke, 1979). These distinct boundary layers represent four topologically different portions of what is known as the magnetospheric boundary layer (or boundary layer for short). The definition of the magnetospheric boundary layer is topologically descriptive and a general consensus on the physics involved in its formation is still lacking (see the review by Lundin, 1988a). From a topological point of view the boundary layer is a region of plasma immediately inside the magnetopause which has predominantly magnetosheath characteristics and tailward/anti-sunward flow. The topological/morphological characteristics of the boundary layer are well described in the article by Lundin (1988a) and need not to be repeated here.

In the Impulsive Penetration Model, the boundary layer is the main site of particles energy and momentum transfer. In the IP model, the frontside magnetospheric boundary layer is considered as the stopper region of all solar wind irregularities with excesses of momentum (Lemaire, 1979a). Eastman *et al.* (1976) suggested that the magnetospheric boundary layer observed by IMP-6 and VELA satellites along the flanks of the magnetosphere is formed by magnetosheath plasma which has diffused into the magnetosphere and which is streaming parallel to the magnetopause across closed magnetospheric field lines. The initial penetration of plasma into the geomagnetic field to produce a relatively thick boundary layer was supposed to proceed by diffusive processes (e.g., Eviatar and Wolf, 1968). The boundary-layer model of Eastman *et al.* (1976), as well as related approaches by Coleman (1970) or Cole (1974) were steady-state models. An important difference between diffusion/viscosity or merging/reconnection models and the impulsive model is that the latter emphasizes the time-dependent processes in the solar wind-magnetosphere interaction as the result of the non-uniformity of the solar wind plasma. There are in fact two kinds of observations which give support to the IP model. The first includes observations made in the boundary layer itself and the second is related to observations made in the polar ionosphere where the signature of an impulsively penetrating plasmoid can be observed.

5.1. Observations of plasma blobs in the magnetospheric boundary layer

The presence of plasma blobs in the magnetospheric boundary layer has been observed by several authors. Sckopke *et al.* (1981) and Lundin and Aparicio (1982) considered the presence in the boundary layer of 'blobs' of high-density magnetosheath – like plasma imbedded in the less dense background boundary-layer plasma. Sckopke *et al.* (1981) suggested that the 'blobs' were either due to temporal modulations of a source of plasma or resulted from a Kelvin–Helmholtz instability. The former interpretation sustains the IP model since impulsive penetration of plasma through the magnetopause results from temporal modulations of the solar wind due to the presence of plasma inhomogeneities embedded in the flow. The PROGNOZ-7 plasma mantle observations (Lundin and Aparicio, 1982) showed that magnetosheath plasma elements locally may penetrate the magnetopause and form high-density, magnetosheath-like regions in the magnetosphere in good agreement with the predictions of the IP model of Lemaire *et al.*

(1979). A meaningful difference in the drift velocity between the magnetosheath ions injected into the boundary layer near noon (He^{++}) and a local plasma population (He^+ and O^+) was inferred from PROGNOZ-7 ion composition (Lundin *et al.*, 1987). Due to this meaningful difference in the drift for various ion species (up to 150 km s^{-1}) it was concluded by Lundin (1984) and Lundin and Dubinin (1984) that the injected magnetosheath plasma in the boundary layer had an excess momentum as compared to the ambient (pre-existing) magnetospheric plasma. In essence, the difference in drifts of individual plasma components was considered as due to the relative motion (with respect to the ambient plasma) of filamentary plasma structures injected from the magnetosheath into the boundary layer.

Bulk plasma flow in the low-latitude boundary layer generally has a large cross-field component (Eastman, 1979). This cross-field flow component will establish a polarization electric field as do also the penetrating solar wind elements. In an attempt to confirm the evidence for reconnection reported by Paschmann *et al.* (1979), Eastman and Frank (1982) have concluded that ISEE observations of the September 8, 1978 magnetopause crossing appear to be most consistent with impulsive injection of magnetosheath plasma across the magnetopause. Three-dimensional observations of plasma flow in the low-latitude boundary layer based on detailed analyses of 18 ISEE-1 magnetopause crossings (Eastman *et al.*, 1985) have been shown to be consistent with $\mathbf{E}_p \wedge \mathbf{B}$ drift imposed by polarization fields $\mathbf{E}_p$ established near the forward extent of penetrating magnetosheath irregularities which are producing the boundary layer. These observations of plasma flow have demonstrated that these polarization fields are present and significant. In addition, Eastman *et al.* (1985) have also observed the field-aligned depolarizing current linking the boundary layer (acting as a generator) to dissipative regions, especially the cusp-region (acting as a load). This basic observation indicates that the plasma boundary layer acts primarily as a generator in a dynamo process in which excess momentum of solar wind plasma irregularities is transferred to the dayside cusp ionosphere (Lemaire and Roth, 1978; Lemaire, 1979a).

5.2. Ionospheric Signatures of Impulsively Magnetosphere Penetrating Plasmoids

Some early observations in the polar cusps contributed to support the impulsive penetration model. An enhancement of the polar cusp ionospheric temperature was observed by Thomas *et al.* (1966), Titheridge (1976), and Whitteker (1976). This temperature enhancement was attributed to the dissipation by Joule heating (Cole, 1971) in the polar cusp ionosphere of the convection kinetic energy of the penetrating element (Lemaire and Roth, 1978).

Carlson and Rorbert (1980) have detected impulsive magnetosheath like plasma precipitation in the low altitude cusp regions with the ion source presumably on closed field lines near the magnetopause.

Goertz *et al.* (1985) were the first to report ground-based data as being the signature of events occurring near the magnetopause that they interpreted as Flux Transfer Events (FTE). What they observed were sporadic and spatially isolated flows in the field of view of STARE, the Scandinavian Twin Auroral Radar Experiment (Greenwald *et al.*, 1978), occurring on time-scales of a few minutes and in regions, which in the ionosphere, range in size from 50 km to 300 km. Mapping this into the boundary layer suggests scale sizes from 0.2 to 2 R_e. But we argued in Section 4.2.15 that these same observations can be interpretated as solar wind plasmoids penetrating the boundary layer in a sporadic and spatially structured manner. The transient flow pattern in the ionosphere on the equatorward side of the cusp 'proper' is observed to turn poleward and anti-sunward. In the theory of impulsive penetration, it is the location where the ionospheric signatures are observed that moves equatorwards, while the ionospheric plasma is driven polewards as the result of mapping the flow pattern surrounding the penetrating plasmoid as discussed in Section 4.2.15.

A similar event was reported by Todd *et al.* (1986) using EISCAT radar data. Other similar events were also reported by Lanzerotti *et al.* (1986, 1987) and Friis-Christensen *et al.* (1988) using ground based magnetometer.

Recently Heikkila *et al.* (1989) have presented a variety of data related to a transient auroral event on the dayside and coming from a large number of sensors, ground-based and aboard spacecraft. These data include observations of magnetic field perturbations by ground-based magnetometers located at different locations in Greenland, Baffin Island, the South Pole, as well as in Northern Europe; of flow patterns by the incoherent scatter radar at Sonderstrom; of auroral activity by all-sky camera photographs at Sonderstrom and by the Polar Bear satellite; of particle fluxes by the VIKING satellite and of magnetic field by the ISEE-2 and IMP-8 satellites recording magnetic disturbances in the solar wind. Heikkila *et al.* (1989) have related this transient ionospheric event to an impulsive penetration of solar wind plasma in the low latitude boundary layer.

6. Conclusions

In this report we have discussed the non-stationary interaction of the solar wind with the Earth's magnetosphere from the point of view of the impulsive penetration theory, originally suggested by Lemaire and Roth in 1976 at an EGS meeting in Amsterdam on the 'Magnetopause Regions'.

This theory is supported by laboratory experiments by Bostick (1956, 1957), Baker and Hammel (1962, 1965), Wessel *et al.* (1988) as well as by Demidenko *et al.* (1966, 1967, 1969, 1972).

It is the observation of the irregular nature of the interplanetary magnetic field that led to the idea of impulsive penetration of solar wind irregularities – or plasmoids – into the magnetosphere. These plasmoids which are almost always present in the solar wind can penetrate inside the geomagnetic field beyond what is considered to be the mean position of the magnetopause.

The interaction of a solar wind plasmoid having an excess density with the magnetosphere depends upon the orientation of the IMF. The physical reason for this effect is the dipole-dipole interaction force between the Earth's dipole and the magnetic dipole moment of the 3-D solar wind plasmoid. Solar wind irregularities with an excess density are attracted toward the inside of both magnetotail lobes when the IMF is northward. For a southward IMF the penetration is favored in the frontside magnetosphere, but not in the magnetotail lobes. The penetration and capture of solar wind plasmoids in the cusps regions is possible for almost any orientation of the IMF. The dipole-dipole force acting on a diamagnetic magnetosheath plasmoid is maximum and directed toward the interior of the magnetosphere at any location in the vicinity of the neutral points where the magnetic field direction in the magnetosheath is antiparallel to the magnetospheric field. When IMF $B_y > 0$, the region of the preferred impulsive penetration of solar wind plasmoids is shifted toward dusk (dawn) with respect to the location of the northern (southern) polar cusp. The direction of these shifts is reversed in both hemispheres when IMF $B_y < 0$.

The actual solar wind plasmoids differ from ideal MHD filaments like those considered by Schindler (1979). For instance, plasmoids are of finite extent and their magnetic flux is interconnected with the interplanetary magnetic flux. A cross-B polarization electric field builds up inside a plasmoid and in its vicinity to keep it moving. Its bulk velocity is shown to change adiabatically across a non-uniform magnetic field. Once the plasmoid has reached the region of closed field lines, behind the mean position of the magnetopause, it is then slowed down non-adiabatically. Its excess convection kinetic energy is mainly dissipated by Joule heating in the lower cusp ionosphere. The rate of energy dissipation is controlled by the value of the integrated Pedersen conductivity.

Most of the B-field signatures observed at the magnetopause, including FTE's, correspond to diamagnetic plasmoids of different shapes and of different origins brought by the solar wind. It is indeed the irregular nature of the solar wind flow which induces rapidly changing and non-uniform boundary conditions over the whole magnetopause. The entry of solar wind plasmoids proceeds without having to postulate any kind of anomalous resistivity and without having to trigger any explosive instabilities.

PROGNOZ-7 ion composition measurements (Lundin *et al.*, 1987) have confirmed that the injected solar wind ions have initially an excess momentum compared to the ambient ions. The measurements have shown evidence for mass loading and differences between the average velocity of injected He^{++} magnetosheath ions and the cold local He^{+} and O^{+} ions. They have also clearly demonstrated that ideal MHD is not applicable to describe processes in the magnetospheric boundary layer. Signatures of impulsively penetrating plasmoids can also be found in the ionosphere. Ionospheric transient flow patterns on the equatorward side of the cusp 'proper' are observed to move poleward and antisunward. In the theory of impulsive penetration this observation results from mapping the flow pattern surrounding a penetrating plasmoid.

Acknowledgements

We wish to thank Prof. M. Nicolet for his continuous support and encouragements. J. Lemaire is also very grateful to his colleagues at the Observatoire de Paris-Meudon for stimulating discussions: D. Hubert, A. Mangeney, C. Harvey, and C. Lacombe are deeply acknowledged for their support and friendliness. Discussions with W. Heikkila and T. Y. Lui have been greatly appreciated.

Appendix 1. The MHD Approximation

A.1. Basic Equations

Work on space plasma physics has often been carried on with ideal MHD equations of an incompressible fluid, i.e.,

$$\frac{\partial \rho}{\partial t} + \nabla \cdot (\rho \mathbf{w}) = 0 , \tag{A.1}$$

$$\rho \frac{\partial \mathbf{w}}{\partial t} + \rho(\mathbf{w} \cdot \nabla)\mathbf{w} = -\nabla p + \mathbf{J} \wedge \mathbf{B} , \tag{A.2}$$

$$\nabla \cdot \mathbf{w} = 0 , \tag{A.3}$$

$$\frac{\partial \mathbf{B}}{\partial t} = \nabla \wedge (\mathbf{w} \wedge \mathbf{B}) , \tag{A.4}$$

$$\nabla \wedge \mathbf{B} = \mu_0 \mathbf{J} , \tag{A.5}$$

$$\nabla \cdot \mathbf{B} = 0 , \tag{A.6}$$

where ρ is the mass density and $\mathbf{w}$ the bulk velocity of the plasma. The pressure is p while $\mathbf{J}$ is the current density and $\mathbf{B}$ the magnetic field. Equation (A.1) is the equation of continuity while Equation (A.2) is the hydrodynamic equation of motion. Equation (A.3) accounts for the incompressibility of the flow. If the plasma is infinitely conducting along the field lines and infinitely resistive across them, then the magnetic field is 'frozen' into the plasma and is 'carried away' with the velocity $\mathbf{w}$ as described by Equation (A.4). Equation (A.5) is the Maxwell equation for the curl of $\mathbf{B}$ for which the displacement current is neglected, μ_0 being the vacuum permittivity. The divergenceless character of $\mathbf{B}$ is given by Equation (A.6).

The first three Equations (A.1)–(A.3) are similar in form with the original hydrodynamic equations of an incompressible fluid. However, in a collisionless magnetized plasma, the pressure tensor does not remain isotropic and, therefore, Equation (A.2) assumes the smallness of the anisotropy.

The MHD approximation comes from Equation (A.4) and it is interesting to recall from which assumptions this equation is deduced. To deduce (A.4), it is first assumed that the electric field ($\mathbf{E}$) is zero along the magnetic field lines, i.e.,

$$\mathbf{E} \cdot \mathbf{B} = 0 . \tag{A.7}$$

This implies also that the magnetic field $\mathbf{B}$ is steady or slowly varying. Secondly, it is also assumed that all the particles drift with the electric drift velocity which therefore is identical with the bulk velocity $\mathbf{w}$.

$$\mathbf{w} = \frac{\mathbf{E} \wedge \mathbf{B}}{B^2} = \mathbf{w}_e = \mathbf{w}_i \ . \tag{A.8}$$

From (A.7) and (A.8), the electric field is

$$\mathbf{E} = -\mathbf{w} \wedge \mathbf{B} \, . \tag{A.9}$$

Using the Maxwell equation

$$\frac{\partial \mathbf{B}}{\partial t} = -\nabla \wedge \mathbf{E} \, ,$$

with **E** given by (A.9), it follows that Equation (A.4) is obtained. This is the usual form of the 'frozen' field approximation. In this approximation, the electric drift (A.8) is the only drift velocity of the plasma. This means that gradient **B** and curvature drifts have been left out. Neglecting these additional drifts, however, is unsatisfactory unless

$$(R_i/L) \ll 1 \, , \tag{A.10}$$

where R_i is the ion gyroradius and L is the scale length for spatial variations of the field (and associated plasma parameters).

A.2. On the relevance of the 'frozen-in' field approximation at the magnetopause

The assumption (A.7) implies that there is no component of the electric field along the magnetic field lines. However, at the locations where the magnetic field lines traverse the 3-dimensional surface of a plasmoid, there is always a charge separation electric field. At these locations, double layers are necessarily formed to maintain the quasi-neutrality within the interface between the plasma inside and outside the plasmoid (Lemaire and Scherer, 1978).

Furthermore, it has been shown by Lundin *et al.* (1987) using PROGNOZ-7 ion composition measurements that the drifts of different ion species in the magnetospheric boundary layer are not equal to each others and differ from 'the convection velocity of magnetic field lines' given by Equation (A.8).

As shown previously, the 'frozen-in' field approximation (A.4) is obtained under the assumption that the electric field reduces to the convection electric field (A.9). However, the actual electric field results from the generalized Ohm's law which can be written (see, for instance, Seshadri, 1973):

$$\frac{\partial \mathbf{J}}{\partial t} = \frac{e}{m_e} \nabla \cdot \mathbf{P}_e + \frac{ne^2}{m_e} (\mathbf{E} + \mathbf{w} \wedge \mathbf{B}) - \frac{e}{m_e} (\mathbf{J} \wedge \mathbf{B}) - \frac{ne^2}{m_e} \mathbf{R} \cdot \mathbf{J} \, . \tag{A.11}$$

In this equation, $\mathbf{P}_e$ is the electron kinetic pressure dyad, n is the number density, e is the magnitude of the electron charge, m_e is the electron mass and **R** is the dyadic resistivity.

It is seen that terms of the generalized Ohm's law (A.11) neglected in the MHD approximation (A.9) include

$$\frac{1}{ne}\mathbf{J} \wedge \mathbf{B}, \qquad \frac{1}{ne}\nabla \cdot \mathbf{P}_e \quad \text{and} \quad \frac{m_e}{ne^2}\frac{\partial \mathbf{J}}{\partial t}.$$

The order of magnitude of these terms has been evaluated by Eastman (1979) as a function of the scale length L for spatial variations of the plasma and field parameters. Considering that

$$\omega_{ce} = eB/m_e, \tag{A.12}$$

$$\omega_{pe}^2 = \frac{ne^2}{m_e \varepsilon_0}, \tag{A.13}$$

$$B \sim \mu_0 JL, \tag{A.14}$$

where ω_{ce} and ω_{pe} are, respectively, the gyro-frequency and the plasma frequency for the electrons while ε_0 and μ_0 are the vacuum permittivity and permeability, respectively, Eastman (1979) has evaluated the ratios X, Y, Z of the electric field due to convection $|\mathbf{w} \wedge \mathbf{B}|$ to the other contributions to the electric field neglected in Equation (A.9), i.e.,

$$\left|\frac{1}{ne}\mathbf{J} \wedge \mathbf{B}\right|, \qquad \left|\frac{1}{ne}\nabla \cdot \mathbf{P}_e\right| \quad \text{and} \quad \left|\frac{m_e}{ne^2}\frac{\partial \mathbf{J}}{\partial t}\right|,$$

respectively. He found

$$\frac{X}{L}\,(\mathrm{m}^{-1}) \sim \frac{1}{L}\, wB\, \frac{ne}{JB} \sim \frac{\omega_{pe}^2 w}{\omega_{ce} c^2}, \tag{A.15}$$

where c is the velocity of light in vacuum.

$$\frac{Y}{L}\,(\mathrm{m}^{-1}) \sim \frac{1}{L}\, wB\, \frac{ne}{|\nabla \cdot \mathbf{P}_e|} \sim \frac{w\omega_{ce} m_e}{kT_e}, \tag{A.16}$$

where kT_e is the electron thermal energy.

$$\frac{z}{L^2}\,(\mathrm{m}^{-2}) \sim \frac{1}{L^2}\, wB\, \frac{ne^2}{m_e\,|\partial \mathbf{J}/\partial t|} \sim (\omega_{pe}/c)^2. \tag{A.17}$$

Taking into account of the following typical values across the magnetopause layer (Eastman, 1979)

$$n \sim 10\ \mathrm{cm}^{-3}, \qquad B \sim 30\ \mathrm{nT}, \qquad w \sim 150\ \mathrm{km\ s}^{-1}, \qquad T_e \sim 100\ \mathrm{eV},$$

for which

$$\omega_{ce} \sim 5.3\ \mathrm{k\ s}^{-1}, \qquad \omega_{pe} \sim 178\ \mathrm{k\ s}^{-1}$$

and

$$X/L \sim 10^{-5}\,(\mathrm{m}^{-1}), \qquad Y/L \sim 4.5 \times 10^{-5}\,(\mathrm{m}^{-1}),$$

$$Z/L^2 \sim 3.5 \times 10^{-7}\,(\mathrm{m}^{-2}).$$

It can be seen from (A.15), (A.16), and (A.17) that the contributions to the electric field neglected in Equation (A.9) become comparable to (or greater than) the convection electric field. (i.e., $X = Y = Z \leq 1$) for scale lengths of the order of (or smaller than) 100 km for the Hall term, 22 km for the pressure gradient term, and 1.7 km for the time-depending term. Such scale lengths for plasma and field variations are often observed within the magnetopause boundary layer whose mean thickness is only a few hundred kilometers. Indeed, scale lengths for significant variations in plasma and field parameters, as determined from high time-resolution magnetic field data, may be as small as 10 km (see, for instance, Eastman and Hones, 1979; Frank *et al.*, 1978). These irregularities are always present and well documented by AMPTE observations with high time (and spatial) resolution (Paschmann *et al.*, 1986). They should not be smoothed out 'for convenience', and cannot be neglected, even in a first approximation, because of their large amplitude. Therefore, at the magnetopause, where these irregularities are always present, terms usually neglected in the generalized Ohm's law become comparable to the convection term due to the electric field. Clearly this invalidates the MHD approach.

This conclusion is even re-inforced if we consider the inner edge of the magnetospheric boundary layer with the following typical values given by Eastman (1979):

$$n \sim 1\ \text{cm}^{-3}, \qquad w \sim 50\ \text{km s}^{-1}, \qquad B \sim 40\ \text{nT}, \qquad T_e \sim 150\ \text{eV},$$

for which

$$\omega_{ce} \sim 7\ \text{k s}^{-1}, \qquad \omega_{pe} \sim 56\ \text{k s}^{-1}$$

and

$$X/L \sim 2.5 \times 10^{-7}\ (\text{m}^{-1}), \qquad Y/L \sim 1.3 \times 10^{-5}\ (\text{m}^{-1}),$$
$$Z/L^2 \sim 3.5 \times 10^{-8}\ (\text{m}^{-2}).$$

Indeed, in this case, the contributions to the electric field neglected in Equation (A.9) become comparable to (or greater than) the convection electric field (i.e., $X = X = Z \leq 1$) for scale lengths of the order of (or smaller than) 4000 km for the Hall term, 75 km for the pressure gradient term and 5 km for the time-depending term. Remembering that typical scale lengths for significant variations in plasma and field parameters within the magnetospheric boundary-layer range between 10 km and 4000 km (Eastman, 1979), it can be concluded that the MHD approximation is even much less appropriate at the inner edge of the magnetospheric boundary layer than it is within the magnetopause layer.

In summary, terms usually neglected in the generalized Ohm's law can become comparable to the convection term due to the electric field. This is due to the presence of large amplitude irregularities whose scale lengths range between 10 km and 4000 km. At the sharp boundaries of these irregularities, finite Larmor radius effects do not represent small corrections and the inequality (A.10) is certainly not satisfied. Clearly this invalidates the MHD assumption of 'frozen-in' field as described by Equation (A.4).

Appendix 2. On the Origin and Usage of the Term 'Plasmoid'

The word 'Plasmon' was originally proposed by Bostick to name the plasma-magnetic entities that he produced in his laboratory experiments. But as mentioned in a footnote by Bostick (1956) the term 'Plasmon' was already allocated to a quantum of plasma-oscillation energy. David Pines (from Princeton University) proposed therefore the term 'plasmoid', which Bostick and other laboratory plasma physicists adopted since 1956. No reason that space plasma physicists should employ a different generic term to designate 'plasma-magnetic field entities'.

This term sometimes has been used in a more restricted meaning as 'toroidal plasma-magnetic entities', i.e., annular plasma structures like those first shown in Bostick's laboratory experiments. Hones *et al.* (1982, 1984) have employed the term 'plasmoid' in this restricted meaning to designate plasma-magnetic structures in the magnetotail that they supposed to be 'closed' toroidal ones. However, it is difficult to determine from measurements along one single spacecraft orbit, whether or not a bundle of magnetic field lines is indeed forming a detached closed loop. There remains the possibility for plasmoids of other kinds: e.g., poloidal, helicoidal, spherical, cylindrical, ...

The list of different categories of plasmoids may be as rich as the list of known hydrodynamic structures or eddies.

We adopt the generic term 'plasmoid' to name plasma irregularities of all kinds and all shapes observed in the solar wind, in the magnetosheath and in the magnetosphere-ionosphere system.

It is instructive to mention here the plasmoid definition given by Linhart (1960) in his book: *Plasma Physics*. According to Linhart a plasmoid is a 'cloud of plasma'. Plasmoids can be generated by electrical discharges and may possess an internal distribution of currents, charges and electric and magnetic fields. Such distributions are the result of the birth-conditions of the plasmoid and of its interaction with the external fields'.

References

Akasofu, S. I., Hones, E. W., Jr., Bame, S. J., Asbridge, J. R., and Lui, A. T. Y.: 1973, *J. Geophys. Res.* **78**, 7257.
Anderson, K. A., Harris, H. K., and Paoli, R. J.: 1965, *J. Geophys. Res.* **70**, 1039.
Aubry, M. P., Kivelson, M. G., and Russell, C. T.: 1971, *J. Geophys. Res.* **76**, 1673.
Aubry, M. P., Russell, C. T., and Kivelson, M. G.: 1970, *J. Geophys. Res.* **75**, 7018.
Axford, W. I.: 1969, *Rev. Geophys. Space Phys.* **7**, 421.
Axford, W. I. and Hines, C. O.: 1961, *Can. J. Phys.* **38**, 1433.
Baker, D. A. and Hammel, J. E.: 1962, *Phys. Rev. Letters* **8**, 157.
Baker, D. A. and Hammel, J. E.: 1965, *Phys. Fluids* **8**, 713.
Baumjohann, W. and Paschmann, G.: 1987, *Phys. Scripta* **T18**, 61.
Beard, D. B.: 1960, *J. Geophys. Res.* **45**, 3559.
Belmont, G. and Chanteur, C.: 1989, *Phys. Scripta* **40**, 124.
Bostick, W. H.: 1956, *Phys. Rev.* **104**, 292.
Bostick, W. H.: 1957, *Phys. Rev.* **106**, 404.
Brekke, A. and Hall, C.: 1988, *Ann. Geophys.* **6**, 361.
Burke, W. J., Kelley, M. C., Sagalyn, R. C., Smiddy, M., and Lai, S. T.: 1979, *Geophys. Res. Letters* **6**, 21.
Burlaga, L. F., Lemaire, J., and Turner, J. M.: 1977, *J. Geophys. Res.* **82**, 3191.

Carlson, C. W. and Torbert, R. B.: 1980, *J. Geophys. Res.* **85**, 2903.
Celnikier, L. M., Harvey, C. C., Jegou, R., Kemp, M., and Moricet, P.: 1983, *Astron. Astrophys.* **126**, 293.
Celnikier, L. M., Muschietti, L., and Goldman, M. V.: 1987, *Astron. Astrophys.* **181**, 138.
Chapman, S. and Ferraro, V. C. A.: 1931a, *Terr. Mag. Atmos. Electr.* **36**, 77.
Chapman, S. and Ferraro, V. C. A.: 1931b, *Terr. Mag. Atmos. Electr.* **36**, 171.
Chapman, S. and Ferraro, V. C. A.: 1932a, *Terr. Mag. Atmos. Electr.* **37**, 147.
Chapman, S. and Ferraro, V. C. A.: 1932b, *Terr. Mag. Atmos. Electr.* **37**, 421.
Cole, K. D.: 1971, *Planetary Space Sci.* **19**, 59.
Cole, K. D.: 1974, *Planetary Space Sci.* **22**, 1075.
Coleman, P., Jr.: 1970, *Cosmic Electrodyn.* **1**, 145.
Cowley, S. W. H.: 1982, *Rev. Geophys. Space Phys.* **20**, 531.
Crooker, N. U.: 1977, *J. Geophys. Res.* **82**, 515.
Crooker, N. U.: 1979, *J. Geophys. Res.* **84**, 951.
Daly, P. W., Keppler, E., and Williams, D. J.: 1979, in B. Battrick and J. Mort (eds.), *Proceedings of Magnetospheric Boundary Layers Conference, Alpbach*, ESA SP-148, p. 137.
Daly, P. W., Saunders, M. A., Rijnbeek, R. P., Sckopke, N., and Russell, C. T.: 1984, *J. Geophys. Res.* **89**, 3843.
Demidenko, I. I., Lomino, N. S., Padalka, V. G., Safranov, B. G., and Sinel'niko, K. D.: 1966, *J. Nucl. Energy, C, Plasma Phys.* **8**, 433.
Demidenko, I. I., Lomino, N. S., Padalka, V. G., Rutkevitch, B. N., and Sinel'nikov, K. D.: 1967, *Soviet Phys.–Techn. Phys.* **11**, 1354.
Demidenko, I. I., Lomino, N. S., Padalka, V. G., Rutkevitch, B. N., and Sinel'nikov, K. D.: 1969, *Soviet Phys. Techn. Phys.* **14**, 16.
Demidenko, I. I., Lomino, N. S., and Padalka, V. G.: 1972, *Soviet Phys.–Techn. Phys.* **16**, 1096.
Dolique, J.-M.: 1963a, *Compt. Rend. Acad. Sci. Paris* **256**, 3984.
Dolique, J.-M.: 1963b, *Compt. Rend. Acad. Sci. Paris* **256**, 4170.
Dungey, J. W.: 1961, *Phys. Rev. Letters* **6**, 47.
Eastman, T. E.: 1979, 'The Plasma Boundary Layer of the Earth's Magnetosphere', Ph.D. Thesis, Ref. LA-7842-T, Los Alamos Sci. Lab., Los Alamos, N.M.
Eastman, T. E. and Frank, L. A.: 1982, *J. Geophys. Res.* **87**, 2187.
Eastman, T. E. and Hones, E. W., Jr.: 1979, *J. Geophys. Res.* **84**, 2019.
Eastman, T. E., Papielawska, B., and Frank, L. A.: 1985, *J. Geophys. Res.* **90**, 9519.
Eastman, T. E., Hones, E. W., Jr., Bame, S. J., and Asbridge, J. R.: 1976, *Geophys. Res. Letters* **3**, 685.
Eviatar, A. and Wolf, R. A.: 1968, *J. Geophys. Res.* **73**, 5561.
Fälthammar, C.-G.: 1973, in A. Egeland, O. Holtet, and A. Omholt (eds.), *Cosmical Geophysics*, Universiteit-forlaget, Oslo.
Farrugia, C. J., Elphic, R. C., Southwood, D. J., and Cowley, S. W. H.: 1987, *Planetary Space Sci.* **35**, 227.
Ferraro, V. C. A.: 1952, *J. Geophys. Res.* **57**, 15.
Frank, L. A., Ackerson, K. L., Decoster, R. J., and Burek, B. G.: 1978, *Space Sci. Rev.* **22**, 739.
Freeman, J. W., Jr., Warren, C. S., and Maguire, J. J.: 1968, *J. Geophys. Res.* **73**, 5719.
Friis-Christensen, E., McHenry, M. A., Clauer, C. R., and Vennerström, S.: 1988, *Geophys. Res. Letters* **15**, 253.
Giovanelli, R. G.: 1946, *Nature* **158**, 81.
Giovanelli, R. G.: 1947, *Monthly Notices Roy. Astron. Soc.* **107**, 338.
Giovanelli, R. G.: 1948, *Monthly Notices Roy. Astron. Soc.* **108**, 163.
Goertz, K., Nielsen, E., Korth, A., Glassmeier, K. H., Haldoupis, C., Hoeg, P., and Hayward, D.: 1985, *J. Geophys. Res.* **90**, 4069.
Greenwaldt, R. A., Weiss, W., and Nielsen, E.: 1978, *Radio Sci.* **13**, 1021.
Haerendel, G., Paschmann, G., Sckopke, N., Rosenbauer, H., and Hedgecock, P. C.: 1978, *J. Geophys. Res.* **83**, 3195.
Hansen, A. M., Bahnsen, A., and D'Angelo, N.: 1976, *J. Geophys. Res.* **81**, 556.
Harvey, C. C., Etcheto, J., and Mangeney, A.: 1979, *Space Sci. Rev.* **23**, 39.
Heikkila, W. J.: 1978a, *Planetary Space Sci.* **26**, 121.
Heikkila, W. J.: 1978b, *J. Geophys. Res.* **83**, 1071.
Heikkila, W. J.: 1982, *Geophys. Res. Letters* **9**, 159.
Heikkila, W. J.: 1990, *Space Sci. Rev.* **53**, 1.

Heikkila, J. W., Jorgensen, T. S., Lanzerotti, L. J., and Maclennan, C. G.: 1989, *J. Geophys. Res.* **94**, 15291.

Heppner, J. P.: 1972, *J. Geophys. Res.* **77**, 4877.

Hones, E. W., J. R., Asbridge, J. R., Bame, S. J., Montgomery, M. D., Singer, S., and Akasofu, S. I.: 1972, *J. Geophys. Res.* **77**, 5503.

Hones, E. W., Jr., Birn, J., Bame, S. J., Paschmann, G., and Russell, C. T.: 1982, *Geophys. Res. Letters* **9**, 203.

Hones, E. W., Jr., Birn, J., Baker, D. N., Bame, S. J., Feldman, W. C., McComas, D. J., Zwickl, R. D., Slavin, J. A., Smith, E. J., and Tsurutani, B. T.: 1984, *Geophys. Res. Letters* **11**, 1046.

Kan, J. R. and Burke, W. J.: 1985, *J. Geophys. Res.* **90**, 4171.

Korth, A., Kremser, G., Wilken, B., Amata, E., and Candidi, M.: 1979, in B. Battrick and J. Mort (eds.), *Proceedings of Magnetospheric Boundary Layers Conference, Alpbach*, ESA SP-148, p. 157.

Kremser, G. and Lundin, R.: 1988, Paper presented at the COSPAR Conference in Helsinki, July 18–29, 1988.

Lanzerotti, L. J., Lee, L. C., Maclennan, C. G., Wolfe, A., and Medford, L. V.: 1986, *Geophys. Res. Letters* **13**, 1089.

Lanzerotti, L. J., Hunsucker, R. D., Rice D., Lee, L. C., Wolfe, A., Maclennan, C. G., and Medford, L. V.: 1987, *J. Geophys. Res.* **92**, 7739.

Lee, C. and Fu, Z. F.: 1985, *Geophys. Res. Letters* **12**, 105.

Lee, L. C. and Kan, J. R.: 1979, *J. Geophys. Res.* **84**, 6417.

Lemaire, J.: 1977, *Planetary Space Sci.* **25**, 887.

Lemaire, J.: 1979a, in W. P. Olson (ed.), *Quantitative Modeling of the Magnetospheric Processes*, AGU, Washington D.C., Geophys. Mongr. Ser., Vol. 21, p. 412.

Lemaire, J.: 1979b, in B. Battrick and J. Mort (eds.), *Proceedings of Magnetospheric Boundary Layers Conference, Alpbach*, ESA SP-148, p. 365.

Lemaire, J.: 1985, *Plasma Phys.* **33-3**, 425.

Lemaire, J.: 1987, in A. T. Y. Lui (ed.), *Magnetotail Physics*, Johns Hopkins University Press, p. 83.

Lemaire, J.: 1989, in P. E. Sandholt and A. Engeland (eds.), *Electromagnetic Coupling in the Polar Clefts and Caps*, Kluwer Academic Publishers, Dordrecht, Holland, p. 27.

Lemaire, J. and Burlaga, L. F.: 1976, *Astrophys. Space Sci.* **45**, 303.

Lemaire, J. and Roth, M.: 1978, *J. Atmospheric Terrest. Phys.* **40**, 331.

Lemaire, J. and Scherer, M.: 1978, *J. Atmospheric Terrest. Phys.* **40**, 337.

Lemaire, J., Rycroft, M. J., and Roth, M.: 1979, *Planetary Space Sci.* **27**, 47.

Linhart, J. G.: 1960, *Plasma Physics*, North-Holland Publ. Co., Amsterdam, 278 p.

Lundin, R.: 1984, *Planetary Space Sci.* **32**, 757.

Lundin, R.: 1988a, *Space Sci. Rev.* **48**, 263.

Lundin, R.: 1988b, *Ann. Geophys.* **6**, 143.

Lundin, R. and Aparicio, B.: 1982, *Planetary Space Sci.* **30**, 81.

Lundin, R. and Dubinin, E.: 1984, *Planetary Space Sci.* **32**, 745.

Lundin, R. and Dubinin, E.: 1985, *Planetary Space Sci.* **33**, 891.

Lundin, R., Stasiewicz, K., and Hultquist, B.: 1987, *J. Geophys. Res.* **92**, 3214.

Lyons, L. R., Killeen, T. L., and Walterscheid, R. L.: 1985, *Geophys. Res. Letters* **12**, 101.

Maezawa, K.: 1976, *J. Geophys. Res.* **81**, 2289.

Meng, C. I. and Anderson, K. A.: 1970, *J. Geophys. Res.* **75**, 1827.

Meng, C. I. and Anderson, K. A.: 1975, *J. Geophys. Res.* **80**, 4237.

Miura, A.: 1987, *J. Geophys. Res.* **92**, 3195.

Nishida, A.: 1989, *Geophys. Res. Letters* **16**, 227.

Ogino, T., Walker, R. J., Ashour-Abdalla, M., and Dawson, J. M.: 1985, *J. Geophys. Res.* **91**, 10835.

Ogino, T., Walker, R. J., Ashour-Abdalla, M., and Dawson, J. M.: 1986, *J. Geophys. Res.* **91**, 10029.

Papamastorakis, I., Paschmann, G., Sckopke, N., Bame, S. J., and Berchem, J.: 1984, *J. Geophys. Res.* **89**, 127.

Parker, E. N.: 1967, *J. Geophys. Res.* **72**, 2315.

Paschmann, G., Haerendel, G., Sckopke, N., Rosenbauer, H., and Hedgecock, P. C.: 1976, *J. Geophys. Res.* **81**, 2883.

Paschmann, G., Papamastorakis, I., Baumjohann, W., Sckopke, N., Carlson, C. W., Sonnerup, B. U. Ö., and Lühr, H.: 1986, *J. Geophys. Res.* **91**, 11099.

Paschmann, G., Sonnerup, B. U. Ö., Papamastorakis, I., Sckopke, N., Haerendel, G., Bame, S. J., Asbridge, J. R., Gosling, J. T., Russell, C. T., and Elphic, R. C.: 1979, *Nature* **282**, 243.
Peterson, W. K., Shelley, E. G., Haerendel, G., and Paschmann, G.: 1982, *J. Geophys. Res.* **87**, 2139.
Pudovkin, M. I. and Semenov, V. S.: 1985, *Space Sci. Rev.* **41**, 1.
Reiff, P. H.: 1982, *J. Geophys. Res.* **87**, 5976.
Reiff, P. H. and Burch, J. L.: 1985, *J. Geophys. Res.* **90**, 1595.
Rosenbauer, H., Grunwaldt, H., Montgomery, M. D., Paschmann, G., and Sckopke, N.: 1975, *J. Geophys. Res.* **80**, 2723.
Roth, M.: 1976, *J. Atmospheric Terrest. Phys.* **38**, 1065.
Roth, M.: 1978, *J. Atmospheric Terrest. Phys.* **40**, 323.
Roth, M.: 1979, in B. Battrick and J. Mort (eds.), *Proceedings of Magnetospheric Boundary Layers Conference, Alpach*, ESA SP-148, p. 295.
Roth, M.: 1981, paper presented at the 4th IAGA Scientific Assembly, Edinburgh, August 3–15, 1981, Abstract: IAGA Bulletin No. 45, p. 414.
Roth, M.: 1984, *La structure interne de la magnétopause*, Mémoires de la Classe des Sciences Acad. Roy. de Belgique, Col. 8, 2e série, T XLIV, Fasc. 7.
Roth, M.: 1986, in R. G. Marsden (ed.), *The Sun and the Heliosphere in Three Dimensions*, D. Reidel Publ. Co., Dordrecht, Holland, p. 167.
Roth, M., Lemaire, J., and Misson, A.: 1990, *J. Comput. Phys.* **86**, 466.
Russell, C. T. and Elphic, R. C.: 1978, *Space Sci. Rev.* **22**, 681.
Russell, C. T. and Elphic, R. C.: 1979, *Geophys. Res. Letters* **6**, 33.
Sandholt, P. E., Deehr, C. S., Egeland, A., Lybekk, B., Viereck, R., and Romick, G. J.: 1986, *J. Geophys. Res.* **91**, 10063.
Schindler, K.: 1979, *J. Geophys. Res.* **84**, 7257.
Schmidt, G.: 1960, *Phys. Fluids* **3**, 961.
Schmidt, G.: 1966, *Physics of High Temperature Plasmas*, Academic Press, New York.
Scholer, M., 1983, *J. Geophys. Res.* **52**, 176.
Scholer, M.: 1988, *Geophys. Res. Letters* **15**, 291.
Scholer, M., Ipavich, F. M., Gloeckler, G., Hovestadt, D., and Kleber, B.: 1981, *J. Geophys. Res.* **86**, 1299.
Sckopke, N.: 1979, in B. Battrick and J. Mort (eds.), *Proceedings of Magnetospheric Boundary Layers Conference, Alpbach*, ESA SP-148, p. 37.
Sckopke, N., Paschmann, G., Haerendel, G., Sonnerup, B. U. Ü., Bame, S. J., Forbes, T. G., Hones, E. W., Jr., and Russell, C. T.: 1981, *J. Geophys. Res.* **86**, 2099.
Seshadri, S. R.: 1973, *Fundamentals of Plasma Physics*, American Elsevier Publ. Co., Inc., New York, 545 p.
Sestero, A.: 1964, *Phys. Fluids* **7**, 44.
Sestero, A.: 1965, *Phys. Fluids* **8**, 739.
Sestero, A.: 1966, *Phys. Fluids* **9**, 2006.
Sibeck, D. G., McEntire, R. W., Lui, A. T. Y., Lopez, R. E., Krimigis, S. M., Decker, R. B., Zanetti, L. J., and Potemra, T. A.: 1987, *J. Geophys. Res.* **92**, 12097.
Sonnerup, B. U. Ö.: 1985, in M. R. Kundu and G. D. Holman (eds.), *Unstable Current Systems and Plasma Instabilities in Astrophysics*, D. Reidel Publ. Co., Dordrecht, Holland, p. 5.
Southwood, D. J.: 1987, *J. Geophys. Res.* **92**, 3207.
Southwood, D. J., Farrugia, C. J., and Saunders, M. A.: 1988, *Planetary Space Sci.* **36**, 503.
Thomas, J. O., Rycroft, M. J., Colin, L., and Chan, K. L.: 1966, in J. Frihagen (ed.), *Electron Density Profiles in the Ionosphere and Exosphere*, North-Holland, Amsterdam, p. 322.
Titheridge, J. E.: 1976, *J. Geophys. Res.* **81**, 3221.
Todd, H. B., Bromage, B. J. I., Cowley, S. W. H., Lockwood, M., van Eyken, A. P., and Willis, D. M.: 1986, *Geophys. Res. Letters* **13**, 909.
Turner, M. J., Burlaga, L. F., Ness, N. F., and Lemaire, J.: 1977, *J. Geophys. Res.* **82**, 1921.
Vasyliunas, V. M.: 1975, *Rev. Geophys. Space Phys.* **13**, 303.
Wessel, F. J., Hong, R., Song, J., Fisher, A., Rostoker, N., Ron, A., Li, R., and Fan, R. Y.: 1988, *Phys Fluids* **31**, 3778.
West, H. I., Jr. and Buck, R. M.: 1976, *J. Geophys. Res.* **81**, 569.
Whipple, E. C., Hill, J. R., and Nichols, J. D.: 1984, *J. Geophys. Res.* **89**, 1508.
Whitteker, J. H.: 1976, *J. Geophys. Res.* **81**, 1279.

Williams, D. T., Fritz, T. A., Wilken, B., and Keppler, E.: 1979, *J. Geophys. Res.* **84**, 6385.
Willis, D. M.: 1975, *Geophys. J. Roy. Astron. Soc.* **41**, 355.
Willis, D. M.: 1978, *J. Atmospheric Terrest. Phys.* **40**, 301.
Zanetti, L. J., Potemra, T. A., Iijima, T., Baumjohann, W., and Bythrow, P. F.: 1984, *J. Geophys. Res.* **89**, 7453.